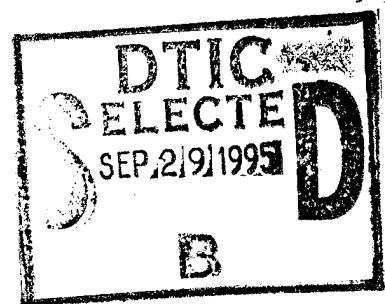
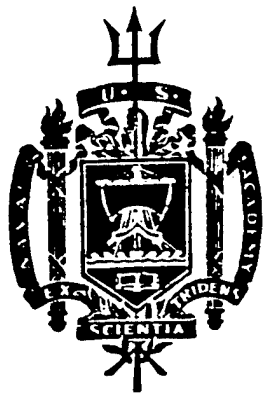


A TRIDENT SCHOLAR PROJECT REPORT

NO. 235

"THE DEVELOPMENT OF AN OPERATIONAL GLOBAL OCEAN CLIMATOLOGY
THROUGH THE USE OF REMOTELY SENSED SEA SURFACE TEMPERATURE"



19950927 151

UNITED STATES NAVAL ACADEMY
ANNAPOLIS, MARYLAND

This document has been approved for public
release and sale; its distribution is unlimited.

DTIC QUALITY INSPECTED 8

DTIC QUALITY INSPECTED 8

REPORT DOCUMENTATION PAGE

Form Approved
OMB no. 0704-0188

Public reporting burden for this collection of information is estimated to average 1 hour of response, including the time for reviewing instructions, searching existing data sources, gathering and maintaining the data needed, and completing and reviewing the collection of information. Send comments regarding this burden estimate or any other aspects of this collection of information, including suggestions for reducing this burden, to Washington Headquarters Services, Directorate for Information Operations and Reports, 1215 Jefferson Davis Highway, Suite 1204, Arlington, VA 22202-4302, and to the Office of Management and Budget, Paperwork Reduction Project (0704-0188), Washington DC 20503.

1. AGENCY USE ONLY (Leave blank)

2. REPORT DATE

3. REPORT TYPE AND DATES COVERED

9 May 1995

4. TITLE AND SUBTITLE The development of an operational global ocean climatology through the use of remotely sensed sea surface temperature

5. FUNDING NUMBERS

6. AUTHOR(S)

Timothy M. Winter

7. PERFORMING ORGANIZATIONS NAME(S) AND ADDRESS(ES)

U.S. Naval Academy, Annapolis, MD

8. PERFORMING ORGANIZATION

REPORT NUMBER USNA

Trident report; no.
235 (1995)

9. SPONSORING/MONITORING AGENCY NAME(S) AND ADDRESS(ES)

10. SPONSORING/MONITORING AGENCY
REPORT NUMBER

11. SUPPLEMENTARY NOTES

Accepted by the U.S. Trident Scholar Committee

12a. DISTRIBUTION/AVAILABILITY STATEMENT

This document has been approved for public release; its distribution is UNLIMITED.

12b. DISTRIBUTION CODE

13. ABSTRACT (Maximum 200 words) Monthly mean satellite-derived sea surface temperature [SST] data have been derived globally using daytime and nighttime AVHRR (Advanced Very High Resolution Radiometer) multi-channel data. From a 12 year data set (1982-1993), valid monthly daytime and nighttime climatologies were created using an eight year subset (1984-1990, 1993). Based on buoy comparisons, four years were omitted due to volcanic aerosol corruption (El Chichón 1982/83, Mt. Pinatubo 1991/92). These resulting monthly climatologies provide SST fields at approximately 1/3rd degree latitude/longitude resolution. Difference fields have been created comparing the new satellite climatology with the older and coarser-resolution climatology constructed from conventional SST data. Regional and zonal climatology differences were also created to highlight the deficiencies, especially in the Southern Hemisphere, in the older climatology believed to result primarily from a lack of buoy/ship (in situ) data. Such comparisons made it clear that the satellite climatology provided a much better product. Ocean current systems, El Niño, La Niña, and other water mass characteristics all appear with better detail and accuracy within the high-resolution satellite climatology.

14. SUBJECT TERMS satellite; sea-surface temperature; climatology

15. NUMBER OF PAGES

16. PRICE CODE

17. SECURITY CLASSIFICATION
OF REPORT

UNCLASSIFIED

18. SECURITY CLASSIFICATION OF
THIS PAGE

UNCLASSIFIED

19. SECURITY CLASSIFICATION OF
ABSTRACT

UNCLASSIFIED

20. LIMITATION OF
ABSTRACT

UNCLASSIFIED

U.S.N.A. --- Trident Scholar project report; no. 235 (1995)

**"THE DEVELOPMENT OF AN OPERATIONAL GLOBAL OCEAN CLIMATOLOGY
THROUGH THE USE OF REMOTELY SENSED SEA SURFACE TEMPERATURE"**

by

Midshipman Timothy M. Winter
United States Naval Academy
Annapolis, Maryland

Tim M. Winter

Certification of Advisors Approval

Adjunct Assistant Professor Alan E. Strong
Department of Oceanography

Alan E. Strong

9 May 95

Associate Professor P.L. Guth
Department of Oceanography

P.L. Guth

9 May 95

Acceptance for the Trident Scholar Committee

Associate Professor Joyce E. Shade
Chair, Trident Committee

Joyce E. Shade

9 May 95

Accession For	
NTIS GRA&I	<input checked="checked" type="checkbox"/>
DTIC TAB	<input type="checkbox"/>
Unannounced	<input type="checkbox"/>
Justification	
By	
Distribution/	
Availability Codes	
Dist.	Avail and/or Special
A-1	

Abstract

Monthly mean satellite-derived sea surface temperature [SST] data have been derived globally using daytime and nighttime AVHRR (Advanced Very High Resolution Radiometer) multi-channel data. From a 12 year data set (1982-1993), valid monthly daytime and nighttime climatologies were created using an eight year subset (1984-1990, 1993). Based on buoy comparisons, four years were omitted due to volcanic aerosol corruption (El Chichón 1982/83, Mt. Pinatubo 1991/92). These resulting monthly climatologies provide SST fields at approximately 1/3rd degree latitude/longitude resolution. Difference fields have been created comparing the new satellite climatology with the older and coarser-resolution climatology constructed from conventional SST data. Regional and zonal climatology differences were also created to highlight the deficiencies, especially in the Southern Hemisphere, in the older climatology believed to result primarily from a lack of buoy/ship (*in situ*) data. Such comparisons made it clear that the satellite climatology provided a much better product. Ocean current systems, El Niño, La Niña, and other water mass characteristics all appear with better detail and accuracy within the high-resolution satellite climatology.

Keywords: satellite, sea-surface temperature, climatology

Table of Contents

Abstract	1
Table of Contents	2
Introduction	3
Objectives and Methods	6
Existing Climatologies	8
Satellite Multi-Channel Sea-Surface Temperature	10
Volcanic Aerosols	14
 MCSST and <i>In-Situ</i> Comparison	 18
i. Satellite Data Collection	18
ii. Buoy and Ship Data Collection	19
iii. Comparison and Validation of Satellite Data	19
 Interpretation of Differences and Anomalies	 23
i. Monthly Differences	23
ii. Monthly Anomalies	24
iii. Yearly Anomalies	27
iv. Regional Differences	30
v. Zonal Differences	39
 Special Examinations	 46
i. El Niño	46
ii. La Niña	47
iii. Areas of Upwelling	52
iv. Current Systems	57
 Conclusions	 63
Acknowledgements	65
References	66
Appendix - Glossary of Terms	68

Introduction

Global climate change has become a lively area of investigation over the past decade. Although there are several ways of monitoring this change, perhaps the most appropriate and accurate lies within the oceans. From 1950 to the late 1970's, *in-situ* data was compiled by Reynolds (1982) to create the National Oceanic and Atmospheric Administration's (NOAA) first operational sea surface temperature (SST) climatology. Previous climatologies of this type have been produced under sponsorship of the Department of Defense (e.g. Robinson, 1976). *In-situ* data are collected by research vessels, stationary buoys, and drifting buoys. Starting in the early 1970's, though, NOAA's polar orbiting satellites began to gather sea surface temperature data through one infrared bandwidth. The introduction of the Advanced Very High Resolution Radiometer (AVHRR), in 1978, allowed the satellites to collect spectral energy through 5 bandwidths (one in the visible range, one in the near-infrared range, and two in the infrared range) (Strong and McClain, 1984). As a result, the products from these data became more accurate and useful. For the past 12 years, the Multi-Channel Sea Surface Temperature (MCSST) data has evolved and become increasingly useful to provide a more detailed and comprehensive way of observing the planet's oceans.

Owing mostly to its global coverage, the satellite has become one of the

most valuable tools in studying the Earth's changing climate. Such platforms monitor many synoptic-scale meteorological and marine phenomena. The present-day NOAA satellites make two complete orbit cycles daily covering the Earth completely every day and night, and collecting 3 to 5 million observations per month compared with 3 thousand by *in-situ* sources (Strong, 1992). By utilizing the AVHRR, the NOAA satellites are capable of accurately measuring sea surface temperatures (SST). These values are recorded from the top 2 μm of the ocean, typically making them a very accurate depiction of the sea's *surface* temperature. The improved SST data allow for scientists to create more accurate models of our oceans and environment. Improved models will assist in all studies involving major current systems, El Niño, sea level rise, and numerous other phenomena.

Several factors need to be considered when attempting to construct a newer, more accurate MCSST-based climatology. First, errors may result from the atmosphere itself. A remote sensing system must "see" through a deep, changing atmosphere to generate its readings. Changing elements such as water vapor, ozone, and aerosols vary in their effect upon the accuracy of the satellite data. Additionally, cloud cover and occasional volcanic eruptions severely impede the operation of the sensors (Strong, 1984).

Due to its greater global coverage, an MCSST climatology and its

coupled anomalies provide significant advantages. A new "model" will provide a way to monitor more effectively global oceanic and atmospheric events such as El Niño. MCSST observations are both more numerous and frequent, thereby, providing more detail when composited than the *in-situ* measurements alone, allowing scientists to assess more accurately other areas of the Earth's oceans that change because of teleconnections with the tropical Pacific's El Niño. Also, major ocean currents can be identified more easily and studied for their year-to-year variabilities. Most importantly, though, a more accurate model would provide a way for studying and more accurately delimiting areas of warming and cooling over the next several decades.

Also, a high-resolution climatology would be of great use to the United States Navy. With a new stress upon littoral and special warfare, an accurate depiction of sea surface temperature and specifically regional departures from "normal", anomalies, could be vital to amphibious operations by providing maximum and minimum temperatures for that region at that time.

Objectives and Methods

This project involved the creation of an up to date/present day, high resolution, satellite sea surface temperature climatology. The MCSST data used in this process are originally compiled and mapped at the University of Miami's Rosenstiel School of Marine and Atmospheric Studies (RSMAS). The SST values are placed into cylindrical equi-rectangular grids of 2048 (longitude) x 1024 (latitude). This corresponds to 18 km of resolution at the equator. These grids were then converted to a smaller 1024 x 512 grid (36 km of resolution), primarily to increase the number of observations per grid location, on the VAX workstations within the USNA/NOAA CPORS (Cooperative Project in Oceanic Remote Sensing) lab at the United States Naval Academy.

In order to establish operational credibility, the MCSST satellite data had to be validated. Gleeson (1994) has recently documented many routine comparisons with both stationary and drifting buoys. A difference of $.1^{\circ}\text{C}$ or less between buoy and satellite data would constitute validation. These comparisons have high relevance to this study; the buoys and their locations are listed in Table I.

Once the data were validated, SST (sea surface temperature) weekly images were manipulated into monthly averages. From 1981 to present, SST data were compiled into daytime and nighttime monthly time series. Based on an eight year subset, 1984-1990 and 1993, monthly, satellite climatology was

created.

Table 1: *Buoy locations used in MCSST comparisons*

25.9N, 89.7W
26N, 93.5W
23.4N, 162.3W
2S, 110W
2N, 110W
8S, 110W
0S, 124W
2N, 140W
0S, 169W
2S, 165E
2N, 165E

The final objective involved the measurement of climatology differences and anomaly charts in order to draw comparisons and outline weaknesses in the present, operational, and conventional climatology. Simply stated, the differences are the result of subtracting Reynolds' climatology from the satellite climatology. Global differences were created on a monthly scale. Then, regional and zonal differences were derived in order to highlight more specific deficiencies in the present, conventional climatology. Anomaly charts, the difference between MCSST observations and a climatology (satellite or Reynolds'), were developed to show how a particular month differs from the overall monthly climatology. Anomalies were measured for every month, throughout the 12 year period, for both the Reynolds and satellite climatology. The identification of all of these differences and anomalies were also accomplished on the VAX stations within the CPORS lab.

Existing Climatologies

The presently preferred, operational climatology was created by Dr. Richard Reynolds of NOAA. From 1950 to the late 1970's, *in-situ* data was collected by Reynolds to create this conventional, coarse resolution, sea surface temperature model (Reynolds, 1982). Ships, stationary buoys, and drifting buoys were all used for the collection of data for his climatology. Within the Northern Hemisphere, buoys and extensive shipping lanes provided good coverage of the northern seas. However, the Southern Hemisphere has fewer buoys and, thus, he relied on shipping lanes for the bulk of the southern data set. Unfortunately, Dr. Reynolds was limited to a little more than 3000 *in-situ* observations per month (Reynolds, 1982). Figure 1 clearly shows the sparsity of data within the Southern Hemisphere.

However, since the launch of the first AVHRR satellite in 1978, many, including Dr. Reynolds, have experimented with ways of properly incorporating the more complete satellite SST data. Presently, he is working on a "blended" climatology of *in-situ* data and satellite MCSST data (Reynolds and Marsico, 1993). This method will allow for real-time correction of any satellite biases relative to the conventional data (Reynolds and Smith, 1994). Unfortunately, though, this correction process degrades the spatial resolution of the product to roughly 1 degree; a satellite MCSST climatology is more accurate, having

a resolution of $1/3$ degrees at the equator.

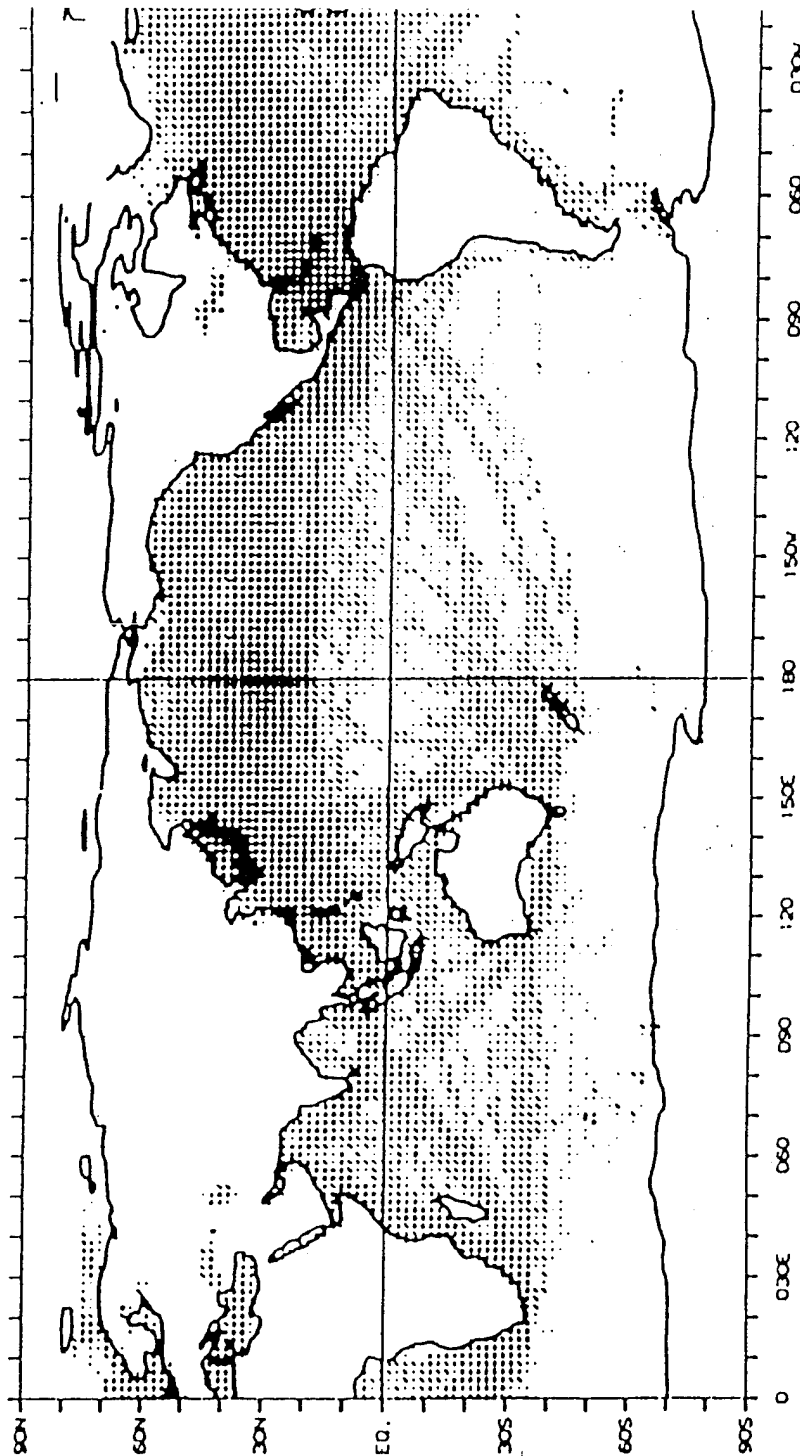


Figure 1. Collection sites of *in-situ* data from stationary buoys, drifting buoys, and ships from one year (Reynolds, 1982).

Satellite Multi-Channel Sea Surface Temperature

The NOAA polar-orbiting satellites circle the earth 14 times per day at an altitude of close to 850 km, allowing for a swath-width of 2600 km (Robinson, 1985). This configuration allows for coverage of the earth's oceans twice daily by each active satellite. The orbiting satellites have been providing over 5 million observations per month uniformly spread throughout the oceans (Strong, 1992). This is dramatically better than the 15000 *in-situ* observations provided by buoys and ships. The difference is especially highlighted in the Southern Hemisphere, where there are fewer buoys and shipping lanes are scarce. Figure 2 shows the satellite coverage difference for March 1989.

Remote sensing of sea surface temperature has become the tool of the oceanographer that has had the largest impact upon marine science over the past decade. In 1978, the first AVHRR (Advanced Very High Resolution Radiometer) system equipped NOAA satellite was launched (Strong, 1991). The AVHRR platform collects radiated energy emitted from the surface of the ocean in five spectral windows, one in the visible spectrum, one in the near-infrared spectrum, and three in the thermal infrared spectrum. The selected atmospheric windows can be seen in Table II (Robinson, 1985).

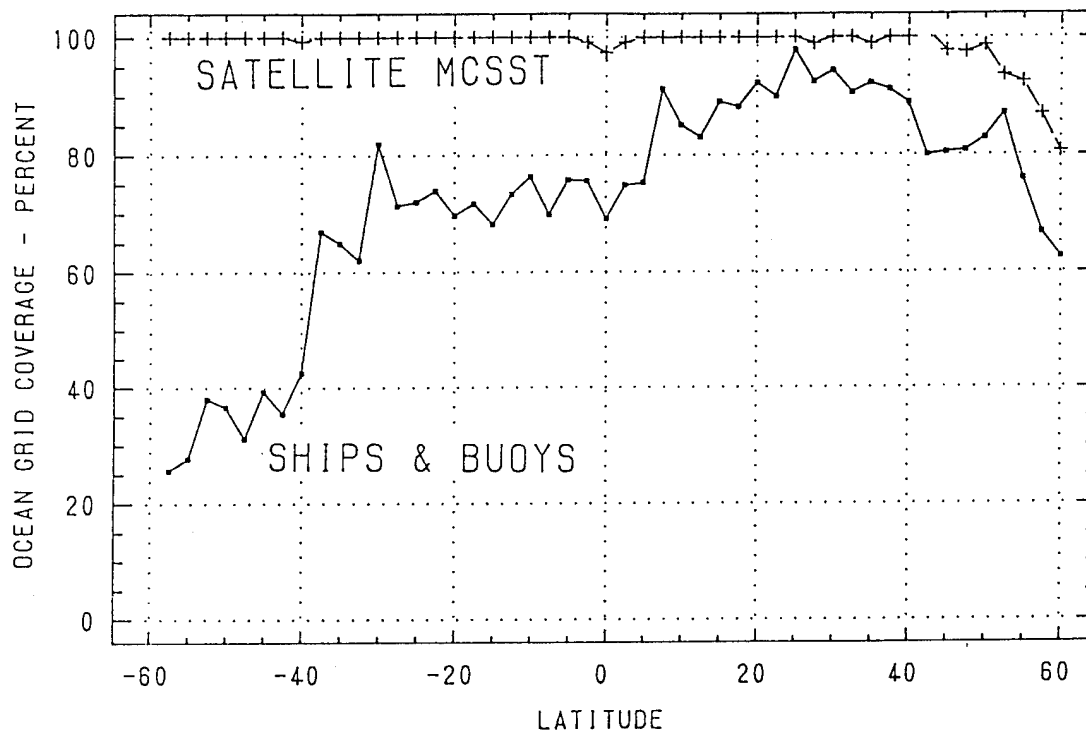


Figure 2. Satellite SST coverage compared with *in-situ* data for March 1989 (Strong, 1992).

Table II. Spectral characteristics of the AVHRR (Robinson, 1985)

Channel	AVHRR	Spectrum
1	.58 - .68 μm	Visible
2	.725 - 1.1 μm	Near -IR
3	3.55 - 3.93 μm	IR
4	10.5 - 11.5 μm	IR
5	11.5 - 12.5 μm	IR

The satellite uses three channels (3,4,5) to measure the radiated temperature (degrees Kelvin) of the top 2 μm of the ocean surface. Combinations of these channels have resulted in empirically derived equations, or algorithms, that allow the removal of attenuating atmospheric water vapor and determine the sea surface temperature in degrees Celsius (Robinson, 1985). The algorithms used by the present NOAA satellite, NOAA 11, are listed in Table III (Strong, 1992).

Table III. Day and Night Algorithms for NOAA-11

Day: $T_s = 3.075T_{11} - 2.0663T_{12} - 264.79$

Night: $T_s = 0.9528T_{3.7} - 0.99T_{11} - 0.9528T_{12} - 269.22$

T_s refers to the final sea surface temperature in Celsius. $T_{3.7}$, T_{11} , and T_{12} represent the brightness temperature values of their respective channels (see Table II). The daytime algorithm excludes the $T_{3.7}$ channel since its proximity to the visible range may cause error due to reflected solar energy. As a result, due to the more accurate algorithm and results from Gleeson (1994), the nighttime MCSST climatology made from only nighttime data is considered to be more reliable.

Even with the creation of such algorithms, cloud effects and atmospheric aerosol contamination remain the greatest cause of error for remotely sensed MCSST data (Gallegos and Hawkins, 1993). As a result, cloud removal

techniques are applied to improve the quality of the satellite SST products. Initially, a low-brightness temperature threshold is established in which a certain pixel of data is deemed to be completely covered by clouds (Robinson, 1985). Any pixel value below this threshold temperature will be discarded as being covered by clouds. Unfortunately, some problems arise when it is too difficult to determine whether an anomalously low temperature results from unmasked cloud coverage or from actual low sea surface temperature. As a result, the visible channels of the AVHRR are used to screen for cloud coverage due to the fact that visible light is highly reflective from the tops of clouds (Robinson, 1985).

During the night, though, the visible channels cannot be used due to the lack of sunlight. In this case, a unique cloud removal process is used. A pixel-by-pixel process compares the difference between three different algorithms, a *split* (11 μ m and the 12 μ m channels), a *dual* (3.7 μ m and 11 μ m channels), and a *triple* (all three channels), and determines the presence of clouds (Robinson, 1985). If the three algorithms agree within a certain empirically predetermined limit, the value can be used and is deemed as cloud free. However, if the three diverge, the pixel value is discarded due to cloud or atmospheric error. Gaps in the data collection created by such elimination are later filled with interpolation as long as no significant horizontal temperature gradients are known to exist within the area.

Volcanic Aerosols

At times, however, the aerosol contamination is so great that the existing algorithms cannot correct for the error. The volcanic eruptions of El Chichón in 1982 and Mt. Pinatubo in 1991 introduced severe amounts of aerosol and volcanic debris into the atmosphere, making the data from these two time periods unusable for the new MCSST climatology (Strong, 1984).

Following an intense volcanic eruption such as these, volcanic debris, sulfuric acid, and aerosols settle above the tropopause and in the stratosphere (20-30 km) (Walton, 1985).. As a result, they are not affected by major weather patterns. Volcanic aerosols, then, may have a residence time ranging from months to years creating an extended period in which SST satellite data cannot be routinely used (Walton, 1985)..

The existence of extensive volcanic aerosols within the stratosphere interferes with the satellite's ability to measure sea surface temperature. The radiation produced by these aerosols is cooler than that of sea surface temperature (Stowe and Strong, 1993). The satellite, thus, receives a radiated temperature that is cooler than the actual sea surface temperature. This causes a temperature depression and creates a negative offset among the satellite data. However, some true cooling of the Earth's oceans does often occur after a volcanic eruption. The magnitude of the cooling, though, is minimal compared to

what the aerosol error implies and, hence, the data remain discarded. Figures 3 and 4 are satellite image anomalies created through a comparison of the contaminated data and the new climatology. It should be noted that NOAA is currently working on creating new volcanic algorithms that will allow for improved corrections to these contaminated data (Stowe and Strong, 1993). Until these MCSST volcanic aerosol contaminated data sets can be corrected, the years 1982, 1983, 1991, and 1992 have been omitted in the production of this high-resolution, satellite-only, SST climatology.

Note: The scales provided for Figure 3 and 4 refer to the anomaly value.

Negative anomalies refer to surface temperature values that are lower than the "normal," while positive anomaly values are sea surface temperatures that are higher than normal. The scales are in °C.



Figure 3. Satellite image anomaly after eruption of El Chichón.



-5 -4 -3 -2 -1 0 1 2 3 4 5

Figure 4. Satellite image anomaly after eruption of Mt. Pinatubo

MCSST and *In-situ* Data Comparison

The new MCSST satellite climatology appears to represent a significant improvement upon the existing, conventional sea surface temperature climatology. Although some have argued that satellite SST data is not accurate enough for certain applications, the resolution benefits and increased number of observations provided by satellite surveillance appear to outweigh many of the still-debated calibration uncertainties (Robinson, 1985). Primarily due to this observation, NOAA has been treating the MCSST product as operational, rather than experimental. One, however, may never depend solely upon a satellite sea surface temperature data set. *In-situ* data (data collected from buoys and ships) must constantly be used in comparison with MCSST data in order to validate the satellite algorithm biases and maintain quality control for the product.

i. Satellite Data Collection

A climatology of the Earth's oceans involves the creation of a model of the true sea-surface temperature. The skin temperature, the temperature found at the very surface of the ocean and at the air-sea interface, is considered by most to be the true sea-surface temperature (Robinson, 1985). Satellite data, collected by the AVHRR, are measured from the radiated energy from the top 2 μm of the ocean surface. This makes it an extremely accurate product for the

creation of a true sea-surface temperature.

ii. Buoy and Ship Data Collection

In-situ (buoy and ship) data collection occurs at various depths. The majority of fixed buoys collect sea-surface temperature data at 1m. Ship data, however, is usually retrieved from ship intakes at various depths (Yokoyama and Tanba, 1991). This may lead to a slight error in a climatology concerned with true "sea-surface" temperature used to model the sea-air temperature interface (Robinson, 1985). Also, one should recall that *in-situ* data collection is reduced in the Southern Hemisphere due to fewer buoys and scarce shipping lanes.

iii. Comparison and Validation of Satellite Data

Gleeson (1994) validated the nighttime MCSST data through comparison with buoy data for a project dealing with coral bleaching. Data was retrieved from NOAA in either hourly or daily measurements and, then, manipulated into weekly values.

Table III summarizes the results of Gleeson's comparison. The average bias of the nighttime MCSST data was found to be less than 0.1°C and the standard error of estimate was 0.5°C . However, it should be noted that the

buoys located at 2N, 110W and 2N, 140W developed problems and were found to repeat inaccurate data causing high biases (Gleeson, 1994).

Also provided are Figures 5,6, and 7 which highlight the Southern Hemisphere comparisons of satellite and buoy data. Figure 8 shows the comparison of MCSST and buoy data after the eruption of Mt. Pinatubo and highlights the drop in MCSST compared to buoy temperature created by the volcanic aerosols.

Table III. Results of buoy/satellite data comparisons
(Gleeson, 1994)

<u>Buoy</u>	<u>Weeks</u>	<u>Std Err</u>	<u>Bias (°C)</u>
25.9N, 89.7W	279	.556	-.042
26N, 93.5W	269	.584	-.087
23.4N, 162.3W	305	.592	-.087
2S, 110W	196	.456	-.087
2N, 110W	207	.689	-.439
8S, 110W	64	.199	-.023
0S, 124W	143	.435	-.018
2N, 140W	184	.474	-.208
0S, 169W	110	.367	.097
2S, 165E	183	.497	-.002
2N, 165E	113	.431	-.005

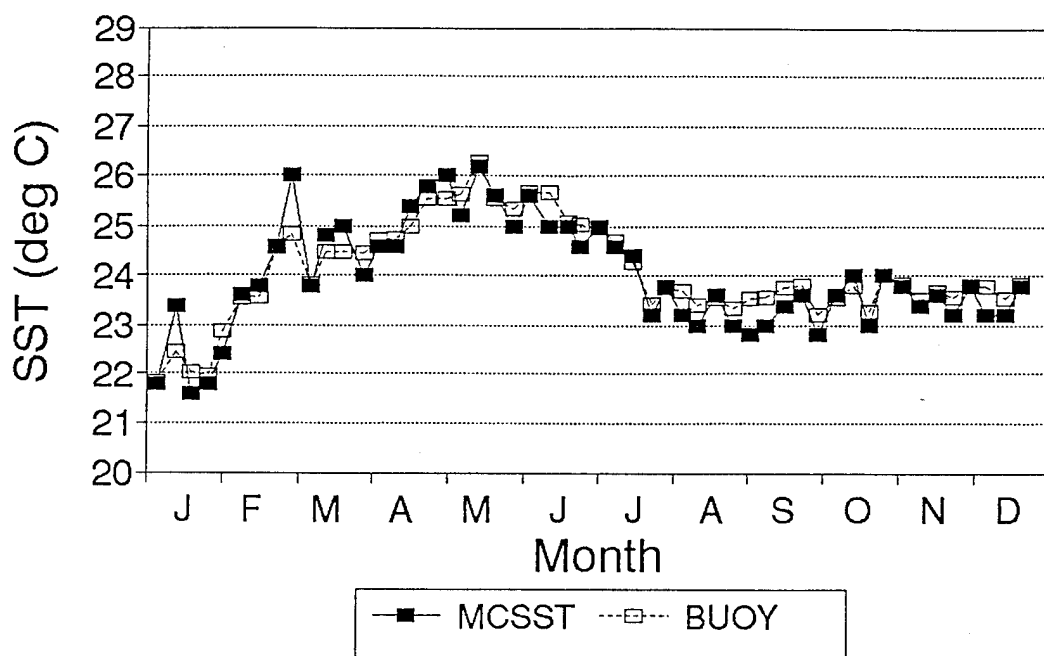


Figure 5. Buoy vs. MCSST weekly comparison at 0S, 124W for 1987 (Gleeson, 1994).

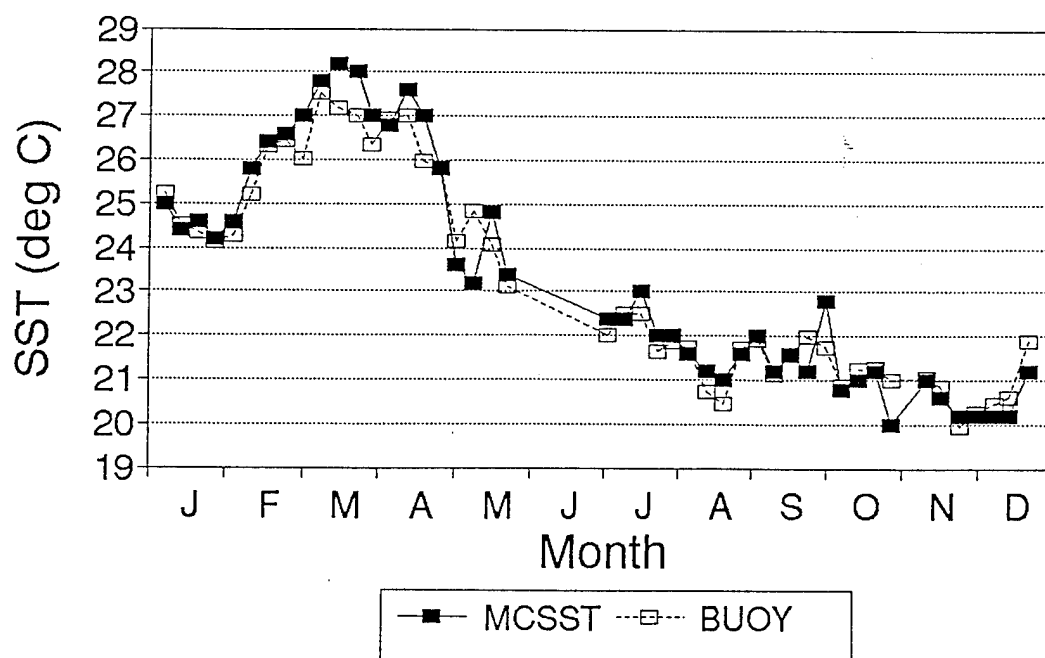


Figure 6. Buoy vs. MCSST weekly comparison at 2S, 110W for 1989 (Gleeson, 1994).

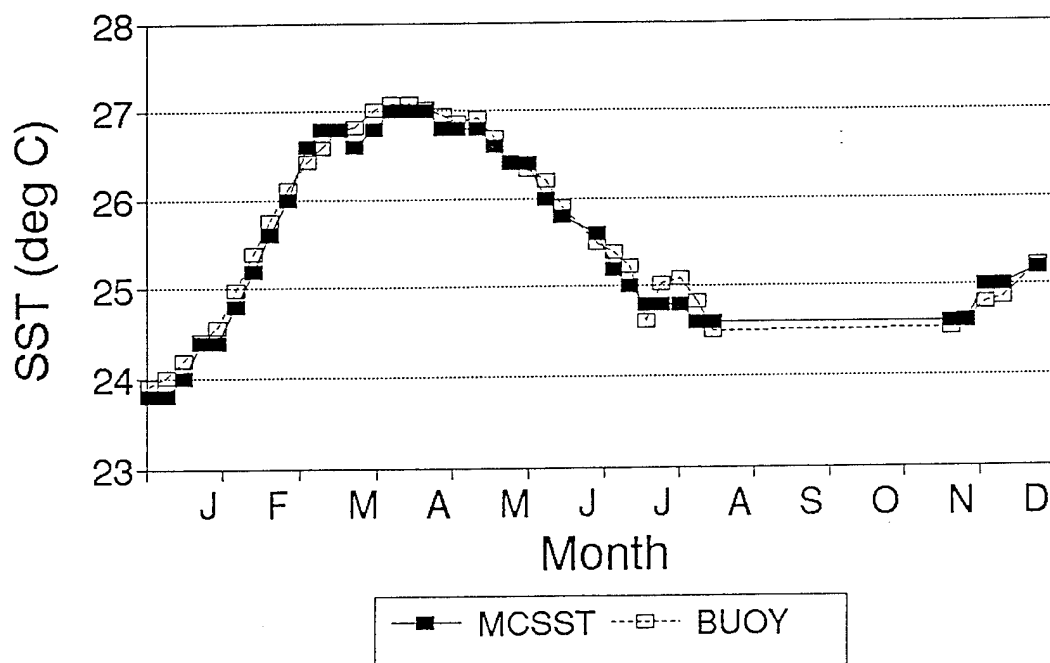


Figure 7. Buoy vs. MCSST weekly comparisons at 8S, 110W for 1986. Missing data from August to November is due to inoperable buoy (Gleeson, 1994).

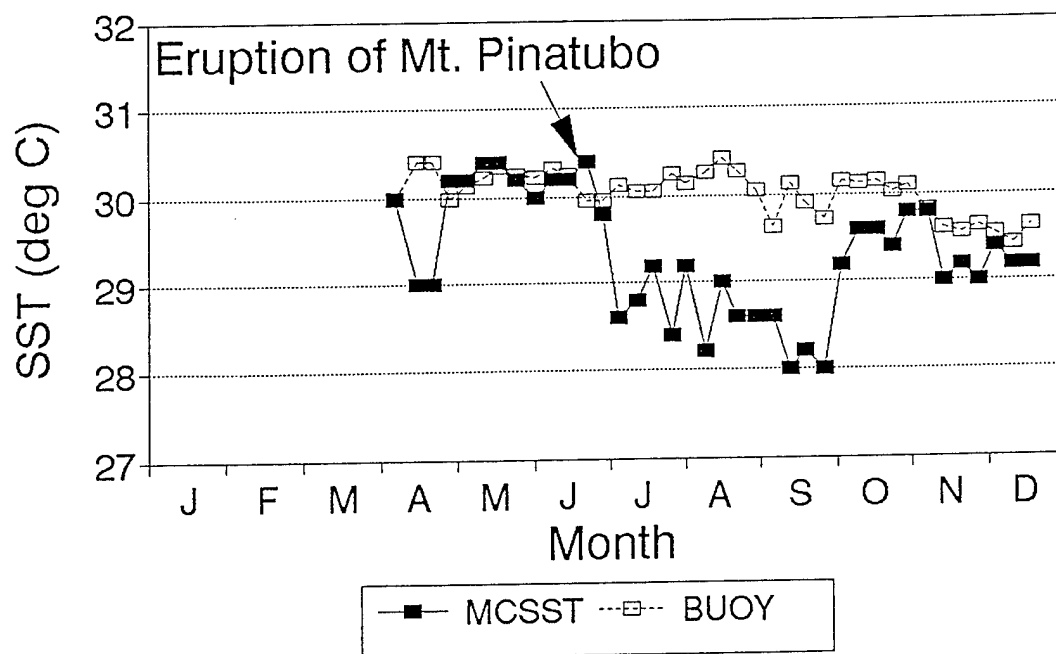


Figure 8. Buoy vs. MCSST weekly comparisons at 2S, 165E for 1991. Notice the results of volcanic contamination leading to a negative offset for months following eruption (Gleeson, 1994).

Interpretation of Differences and Anomalies

In order to completely analyze the new climatology, many difference and anomaly charts were created. Differences show deviations between two climatologies. Such charts become extremely useful when comparing the new MCSST climatology with the Reynolds *in-situ* climatology. Also, areas of weakness and insufficient data can be located by interpreting "difference" results. Anomaly products allow one to see when sea surface temperatures differ from the mean within a particular climatology. Anomaly charts are also used to highlight El Niño and other marine phenomena that cause the sea surface temperature to differ from the norm.

i. Monthly Differences: Satellite Climatology vs. Reynolds' Climatology

First, a set of monthly climatology differences were created. The monthly averages for Reynolds' *in-situ* climatology (created from interpolation between *in-situ* data points) were subtracted from the new MCSST climatology (created from interpolation between satellite data points). Positive values show that the temperature values for every month are warmer within the MCSST climatology. That the anomalies are all positive, is possibly due to the fact that the 1980's and early 1990's, the time period for the new climatology, have been relatively warmer than the previous three decades used by Reynolds (Bates and Diaz, 1991). Results can be seen in Table IV.

Table IV. Monthly difference between the new MCSST climatology and Reynolds' climatology

<u>Month</u>	<u>Difference (°C)</u>
JAN	0.19
FEB	0.29
MAR	0.41
APR	0.37
MAY	0.37
JUN	0.31
JUL	0.29
AUG	0.28
SEP	0.30
OCT	0.24
NOV	0.16
DEC	0.08
<i>Average :</i>	<i>0.27</i>

ii. Monthly Anomalies: MCSST vs. Satellite and Reynolds' Climatologies

Monthly anomalies were created by subtracting each month of every year of both the new MCSST and Reynolds' climatologies from the actual MCSST monthly averages. The results simply highlight the difference between the two climatologies shown in Table IV. In Figure 9, the graph of this anomaly set can be seen. One should notice large anomalies around 1982-83 (negative), 1987-88 (positive), and in 1991-92 (negative). The negative anomalies in late 1982 and 1983 and 1991 and 1992 were mostly due to contaminated MCSST data resulting from the volcanic eruptions of El Chichón and Mt. Pinatubo, respectively. The large positive anomaly in 1987 and early 1988 is due to an El

Niño and results from elevated sea surface temperature (see discussions for further details on page 46).

Anomalies were then derived for both the Northern and Southern Hemispheres using Reynolds' climatology. Graphs are provided in Figures 10 and 11, respectively. Here, it becomes very apparent that extreme yearly variability in the anomalies exist over the Southern Hemisphere. Also, an indication is seen that an overall bias appears to exist between MCSST data and Reynolds' climatology that is greater in the Southern Hemisphere. This will be examined later. It is proposed that the variability and bias result from the lack of *in-situ* data within Reynolds' climatology and shows clearly why improvements upon his climatology are needed.

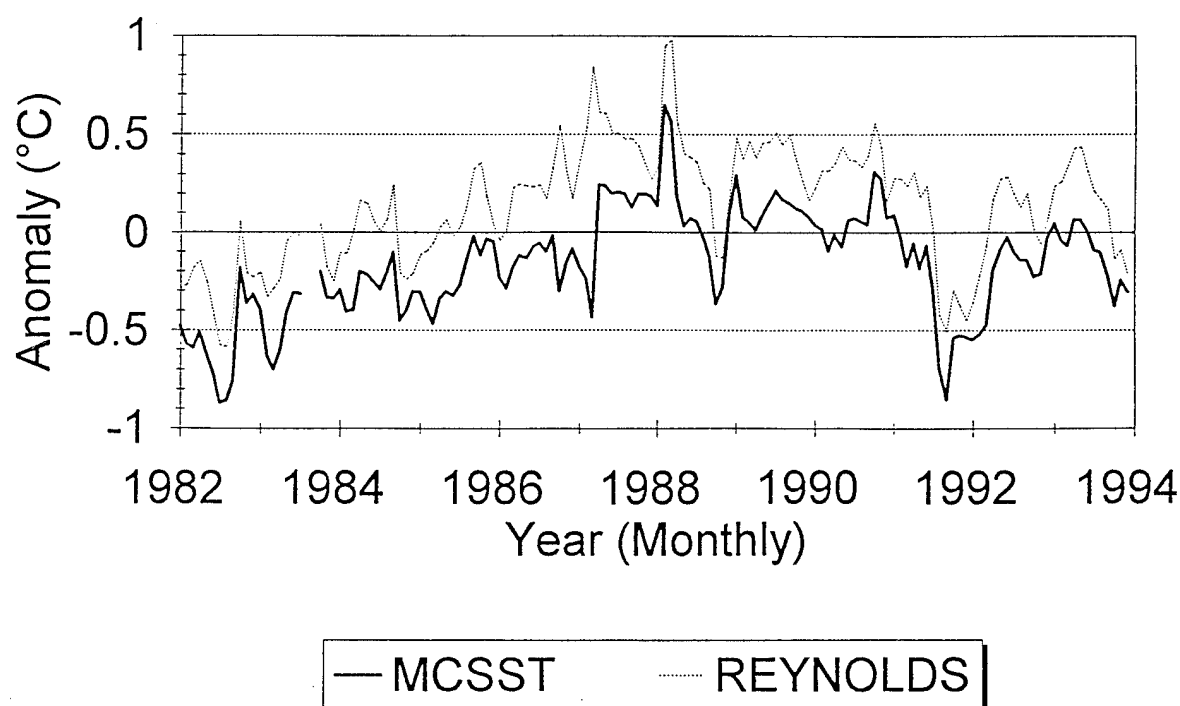


Figure 9. Monthly anomalies for both MCSST vs. Satellite climatology and MCSST vs. Reynolds climatology [Sep. and Oct. 1983 data not available].

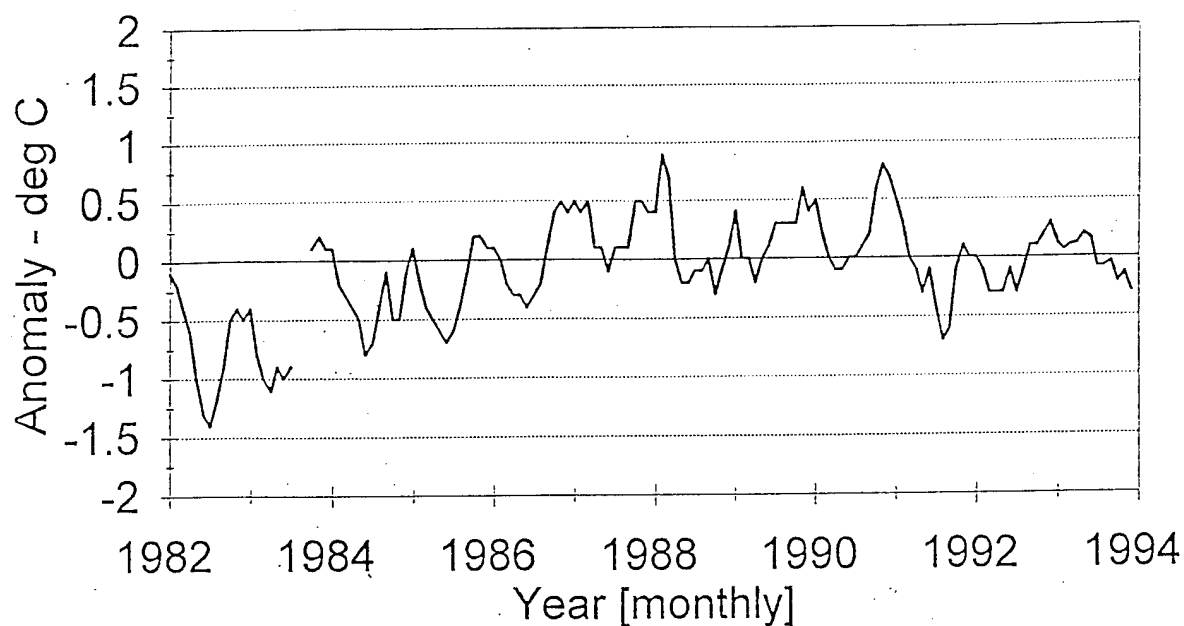


Figure 10. Monthly anomalies (MCSST observations vs. Reynolds' climatology) for the Northern Hemisphere [Sep. and Oct. 1983 data not available].

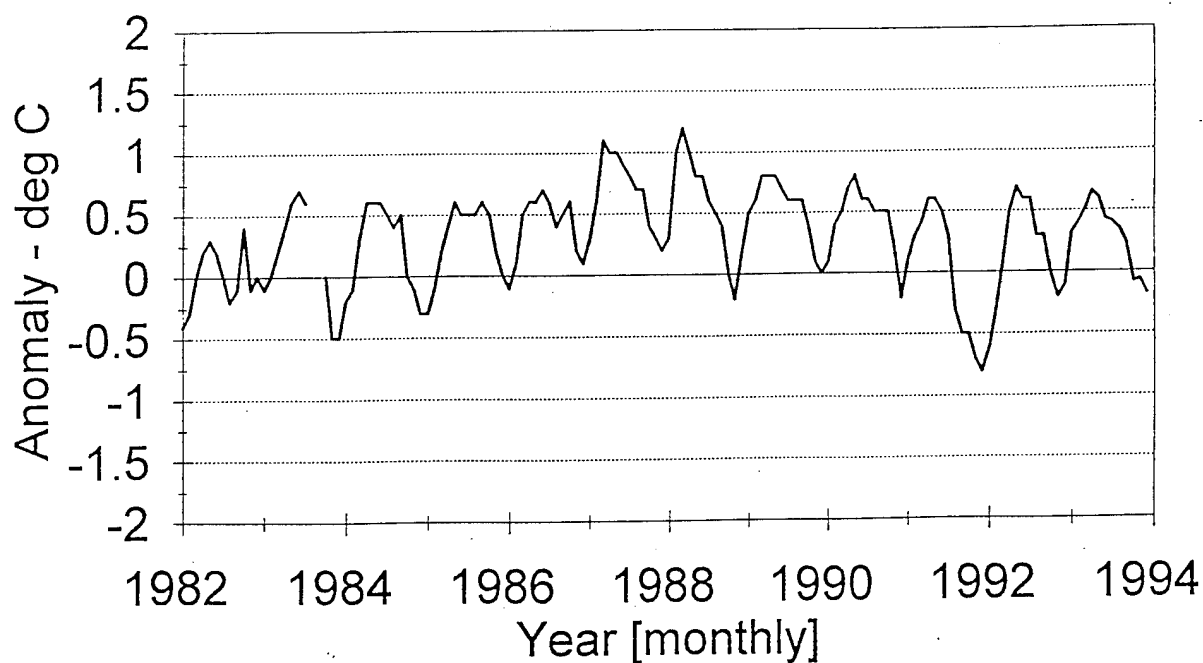


Figure 11. Monthly anomalies (MCSST observations vs. Reynolds' climatology) for the Southern Hemisphere [Sep. and Oct. 1983 data not available]

ii. Yearly Anomalies: MCSST vs. Reynolds' Climatology

In order to eliminate the cyclical nature shown in Figures 10 and 11 (due to the seasons or possibly a ship sampling error) of the monthly anomalies against the Reynolds climatology, yearly anomalies were created between the new climatology and Reynolds'. With these values, it is easier to identify trends and periods of larger anomalies. In Table V, the data is provided for the yearly anomalies in both the Northern and Southern Hemispheres at night and during the day. It is apparent that the Northern Hemisphere values are consistent with global phenomena by having a negative anomaly during the volcanic eruptions (1982 and 1991) and positive values during the El Niño event of 1987. Figure 12 is a graph of the Northern Hemisphere values.

However, the yearly average anomalies in the Southern Hemisphere, shown in Figure 13, are all positive and only show reduced offsets for the volcanic eruptions. The positive magnitude of the anomalies are also greater than those of the Northern Hemisphere. With this in mind, it is clear that the difference between the two climatologies basically results from strong, positive anomalies in the Southern Hemisphere. Once again, this highlights the apparent deficiencies of *in-situ* data within the Southern Hemisphere since there is no obvious reason for such an imbalance in the Southern Hemisphere.

Nighttime MCSST data demonstrate a lower bias and greater accuracy

when compared to *in-situ* measurements. As a result, in both Figures 12 and 13, anomalies created with nighttime MCSST data are closer to zero and define a tighter field.

Table V. Numerical values for yearly MCSST anomalies based on Reynolds' climatology for day and night in both hemispheres.

YEAR	DAY (NH)	NIGHT (NH)	DAY (SH)	NIGHT (SH)
1982	-0.642	-0.708	0.242	0.000
1983	-0.280	-0.570	0.360	0.140
1984	-0.283	-0.367	0.517	0.233
1985	-0.108	-0.242	0.400	0.300
1986	-0.025	-0.017	0.383	0.400
1987	0.308	0.267	0.875	0.667
1988	0.117	0.092	0.925	0.550
1989	-0.008	0.208	0.375	0.542
1990	0.333	0.242	0.583	0.433
1991	-0.083	-0.117	0.392	-0.000
1992	0.083	-0.067	0.492	0.158
1993	0.609	-0.006	0.981	0.302

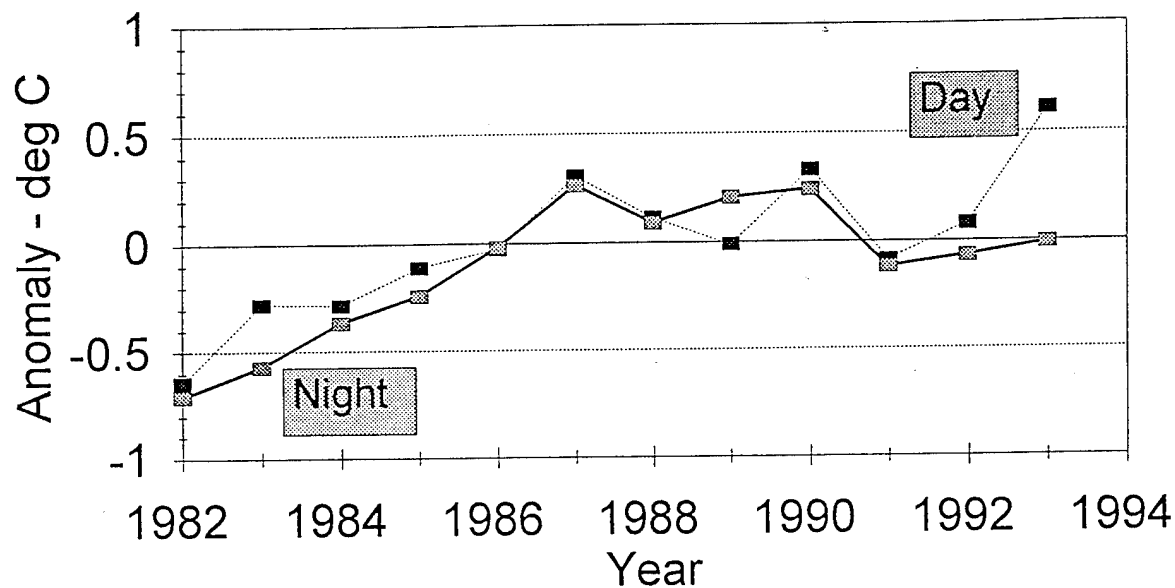


Figure 12. Day and night yearly anomalies (MCSST observations vs. Reynolds' climatology) for the Northern Hemisphere.

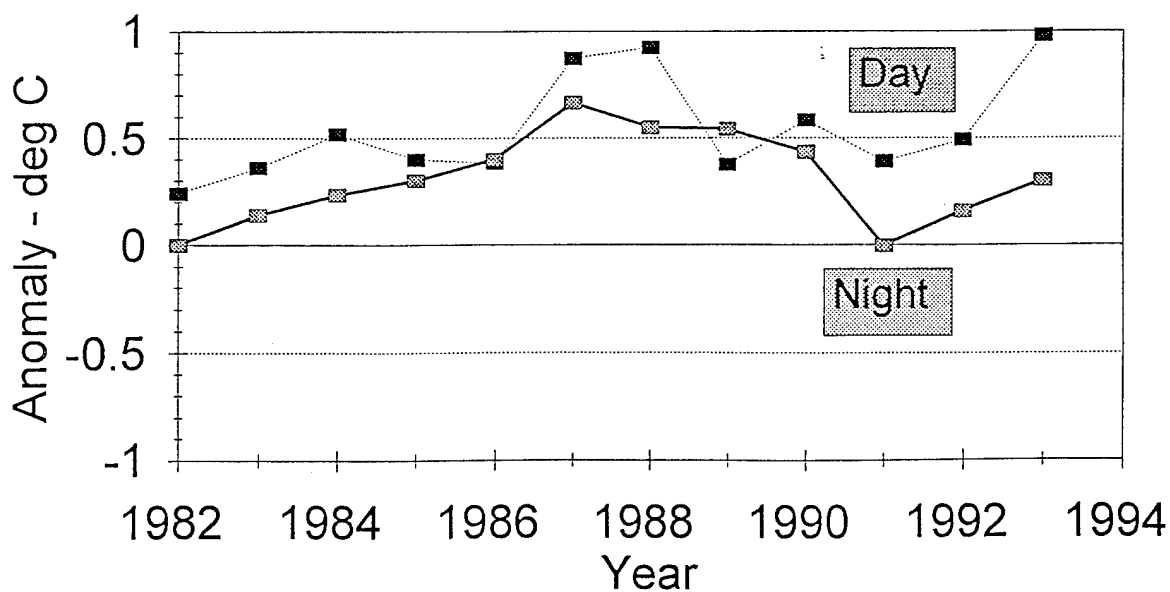


Figure 13. Day and night yearly anomalies (MCSST observations vs. Reynolds' climatology) for the Southern Hemisphere.

iii. Regional Differences: Satellite Climatology vs. Reynolds' Climatology

Regional differences of each major ocean basin were created to further investigate the differences between the satellite and Reynolds' climatology. Masks were created with the VAX workstation to isolate the data within each ocean: North Atlantic, North Pacific, South Atlantic, South Pacific, and Indian Ocean. The masks are presented in Figures 14, 15, 18, 19, and 22. The resulting differences found in these different regions were consistent with previous discoveries and further amplify them. The differences for the North Pacific and the North Atlantic (Figures 16 and 17) were smaller than those of the southern oceans and the Indian Ocean. Also, the northern oceans showed the same pattern of having negative differences from May to July while having positive values for the rest of the year. The negative differences occur during the "warm up" of the Northern Hemisphere in which the air temperature is warmer than that of the water. This may cause error in ship collection of *in-situ* data, making the water appear warmer than it truly is. However, more investigation is required to determine the cause for the negative offsets during those months.

Within the southern and Indian ocean basins (Figures 20, 21, and 23), the differences were all positive and consistent with the positive difference noted in Table IV (page 24). The greatest differences exist within the South Atlantic, which may result from this particular ocean basin having the greatest insufficiency of *in-situ* data.



Figure 14. Image mask for the North Atlantic Ocean.

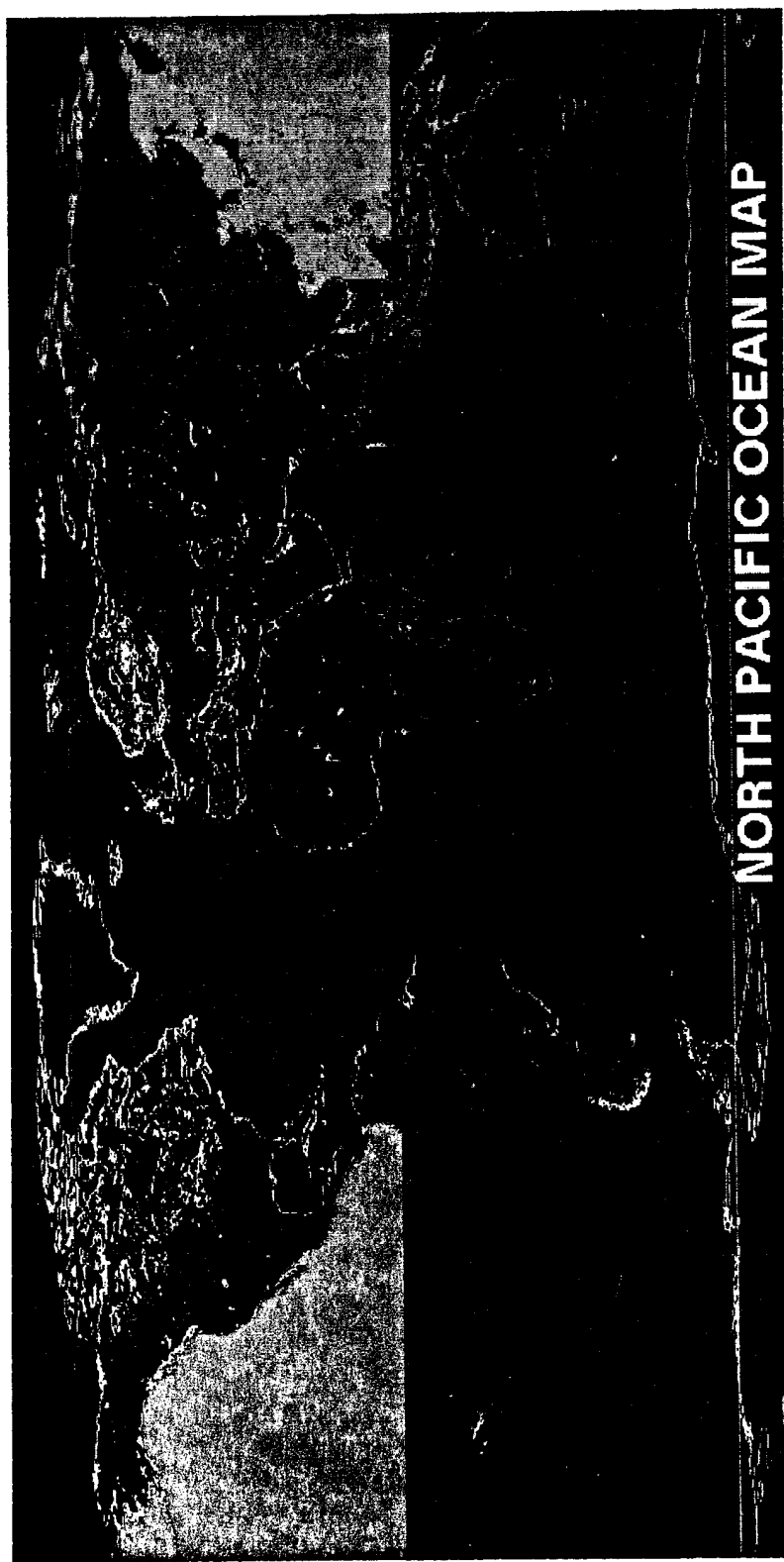


Figure 15. Image mask of the North Pacific Ocean.

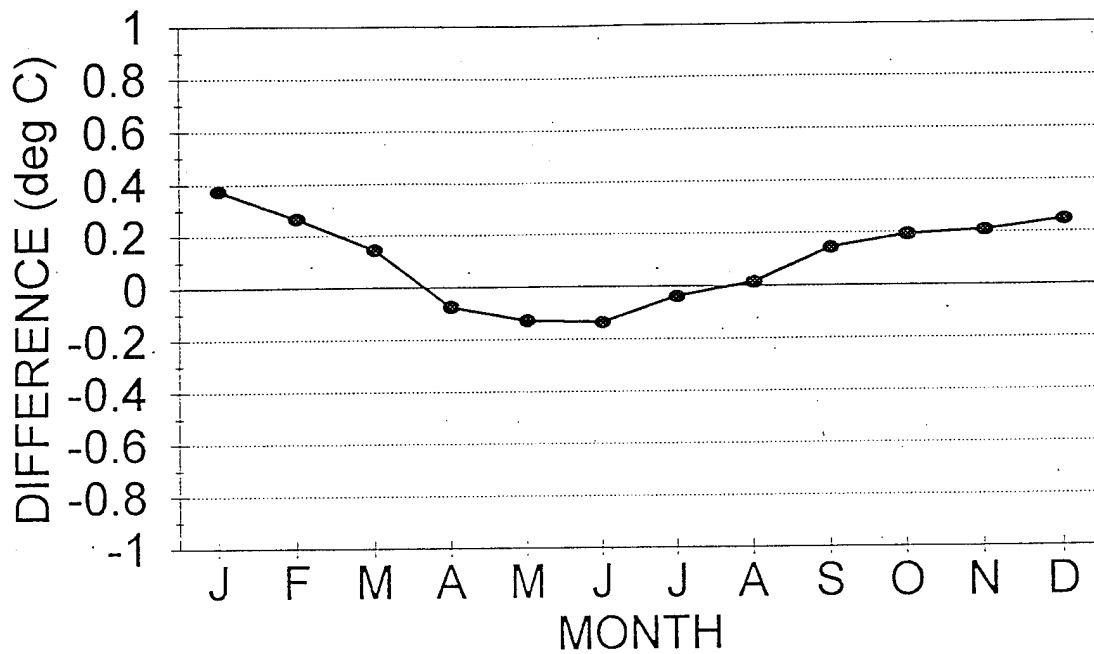


Figure 16. Satellite vs. Reynolds' climatology differences by month for the North Atlantic Ocean.

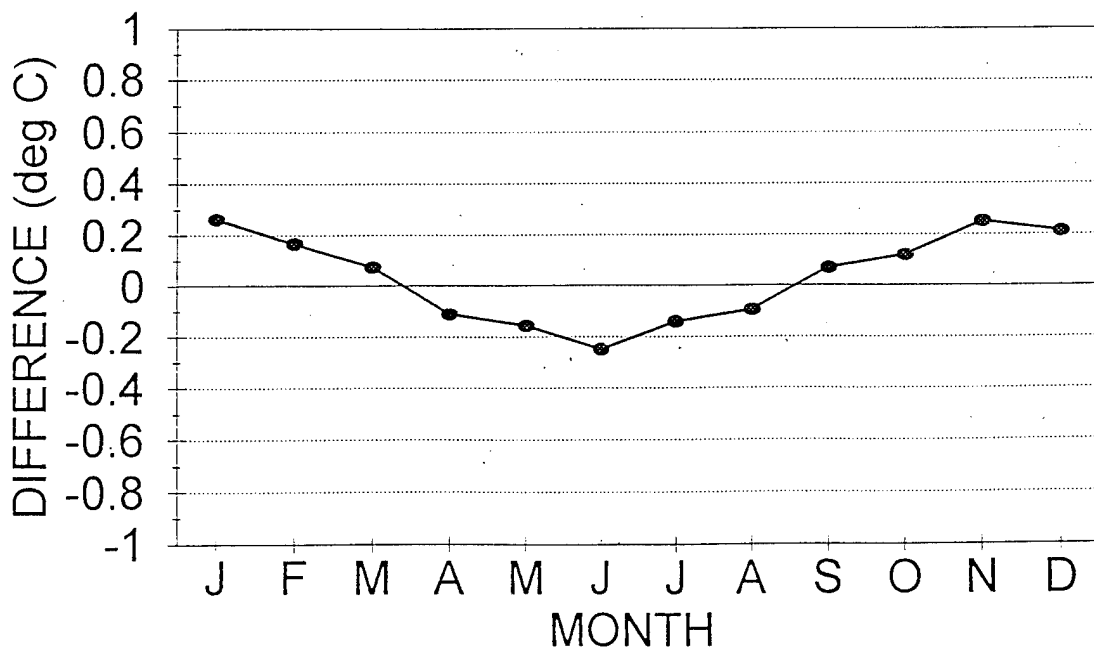


Figure 17. Satellite vs. Reynolds' climatology differences by month for the North Pacific Ocean.

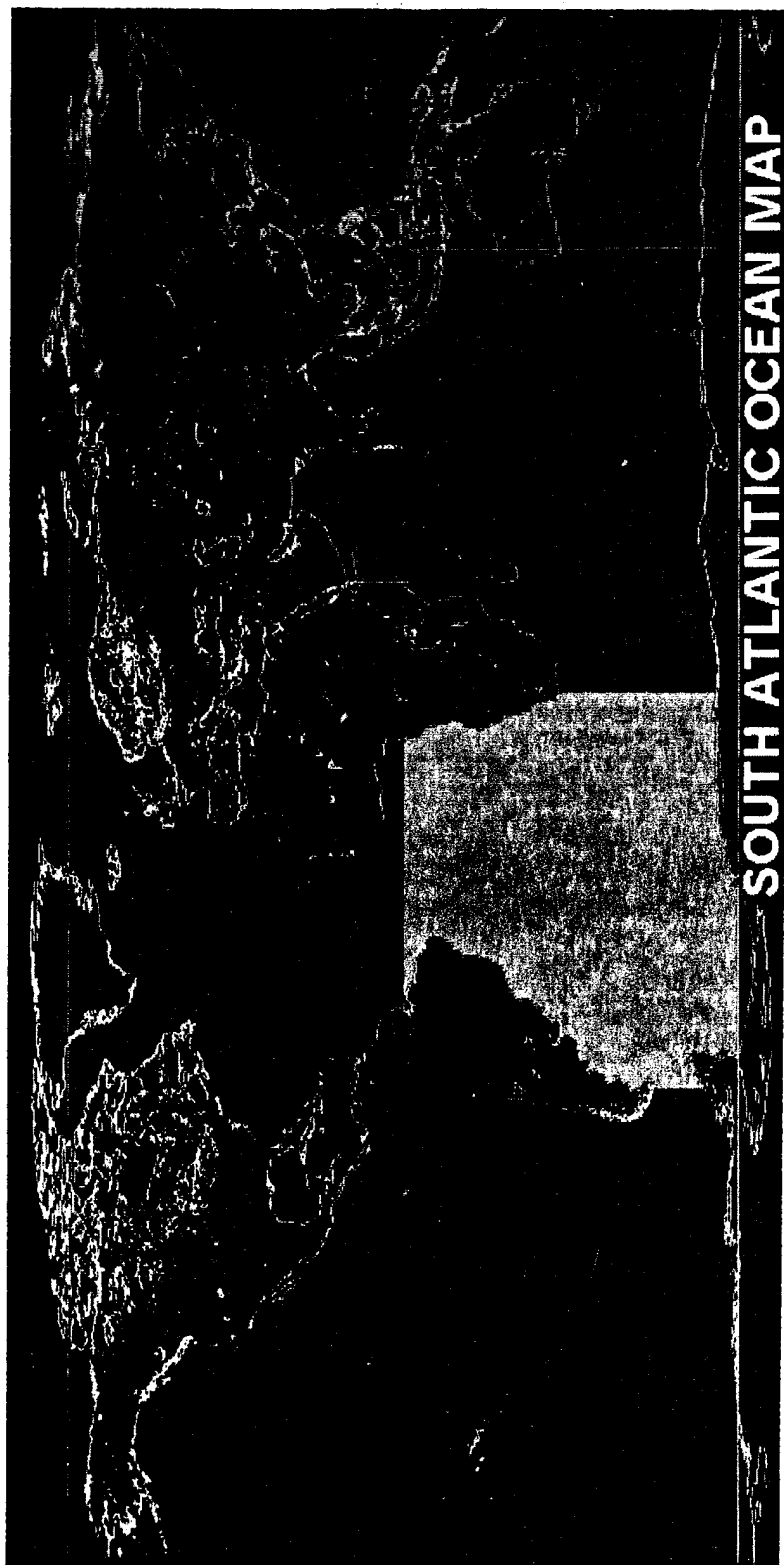


Figure 18. Image mask for the South Atlantic Ocean.

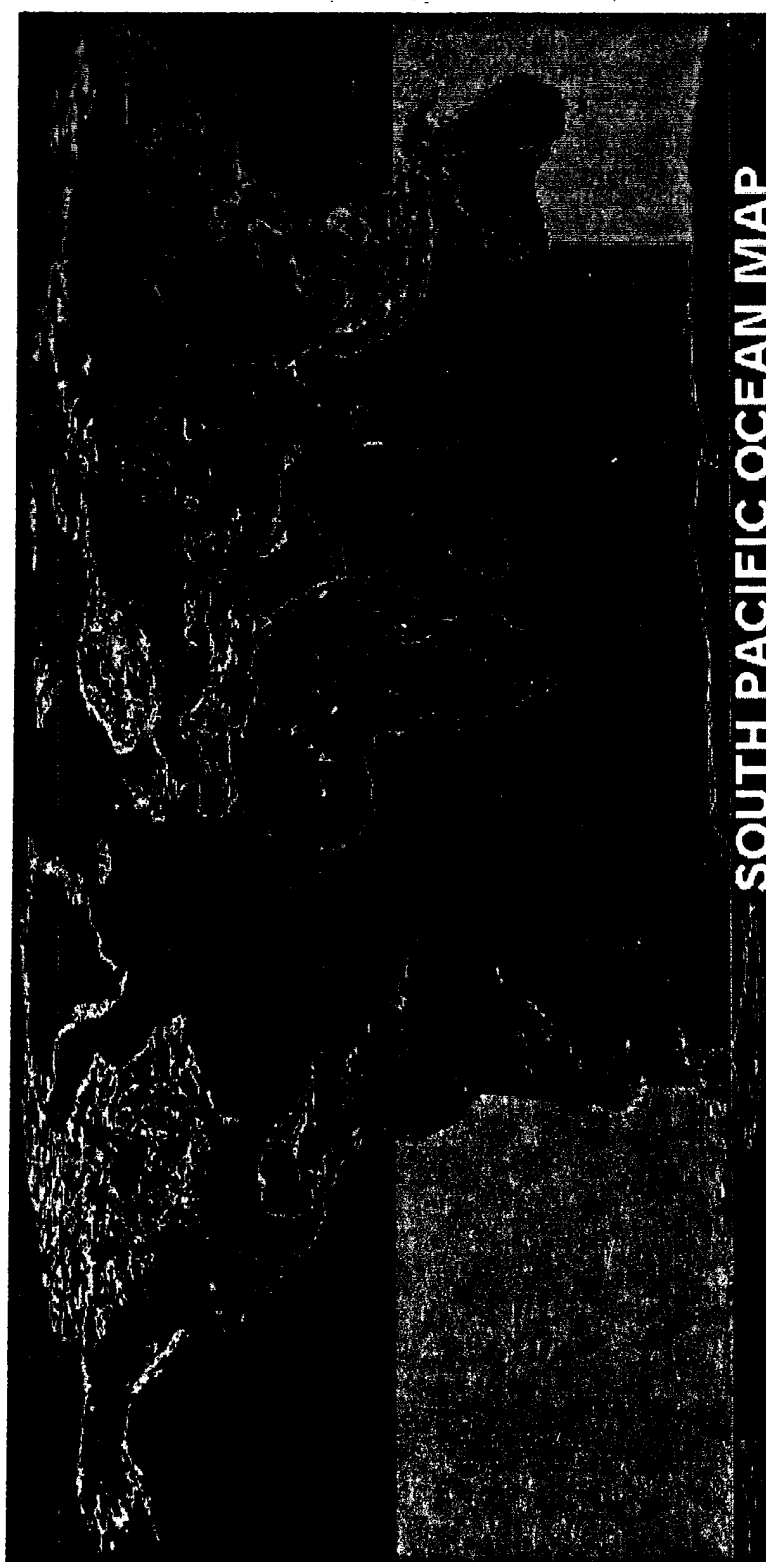


Figure 19. Image mask for the South Pacific Ocean.

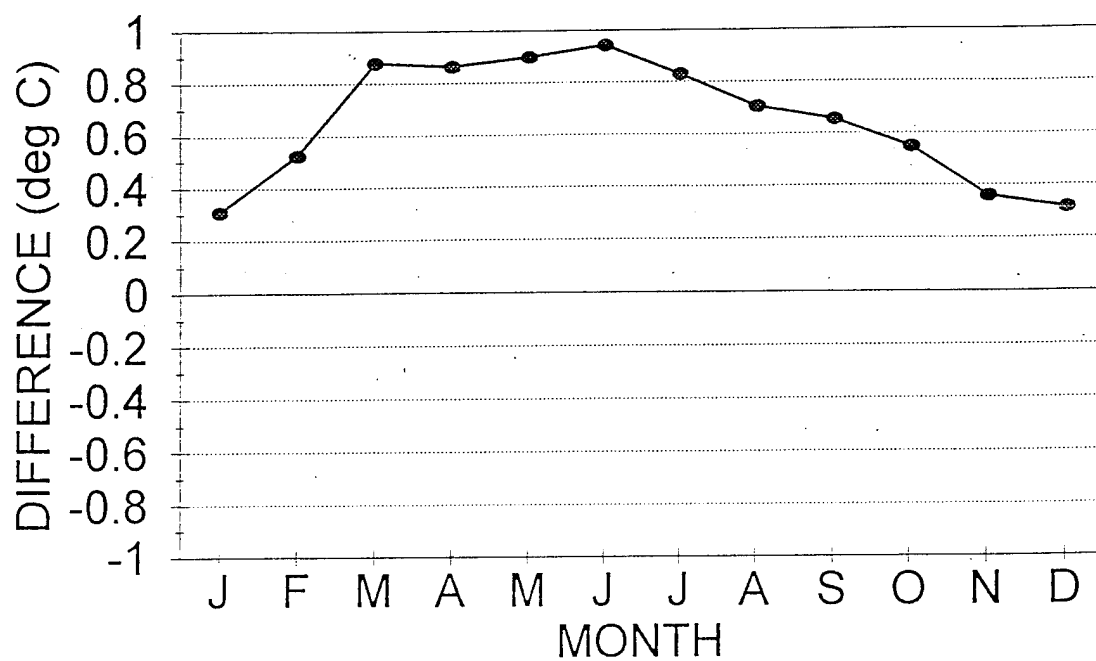


Figure 20. Satellite vs. Reynolds' climatology differences by month for the South Atlantic Ocean.

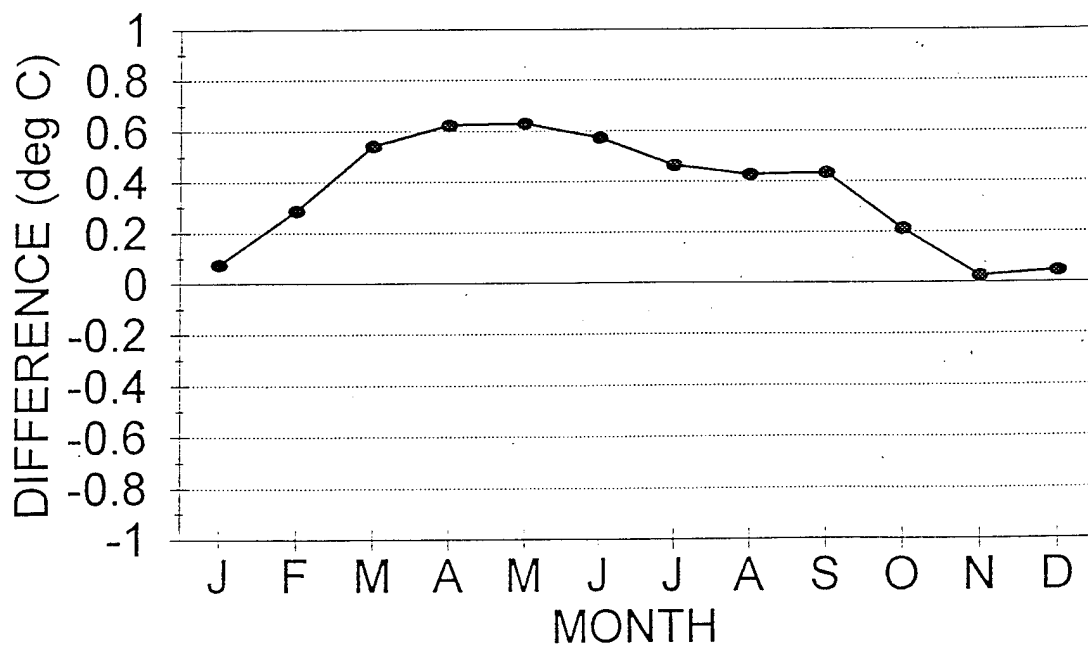


Figure 21. Satellite vs. Reynolds' climatology differences by month for South Pacific Ocean.

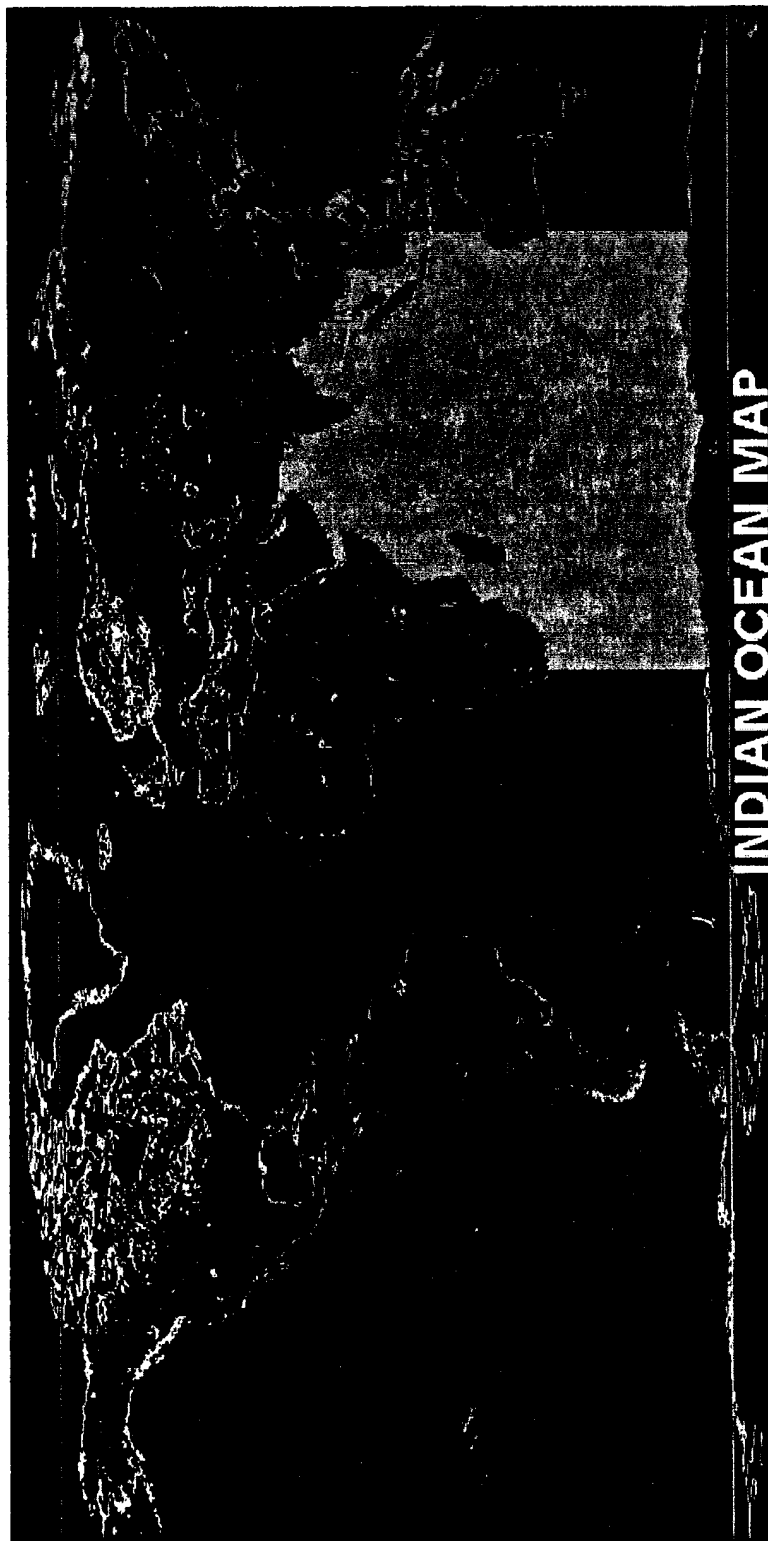


Figure 22. Image mask for the Indian Ocean.

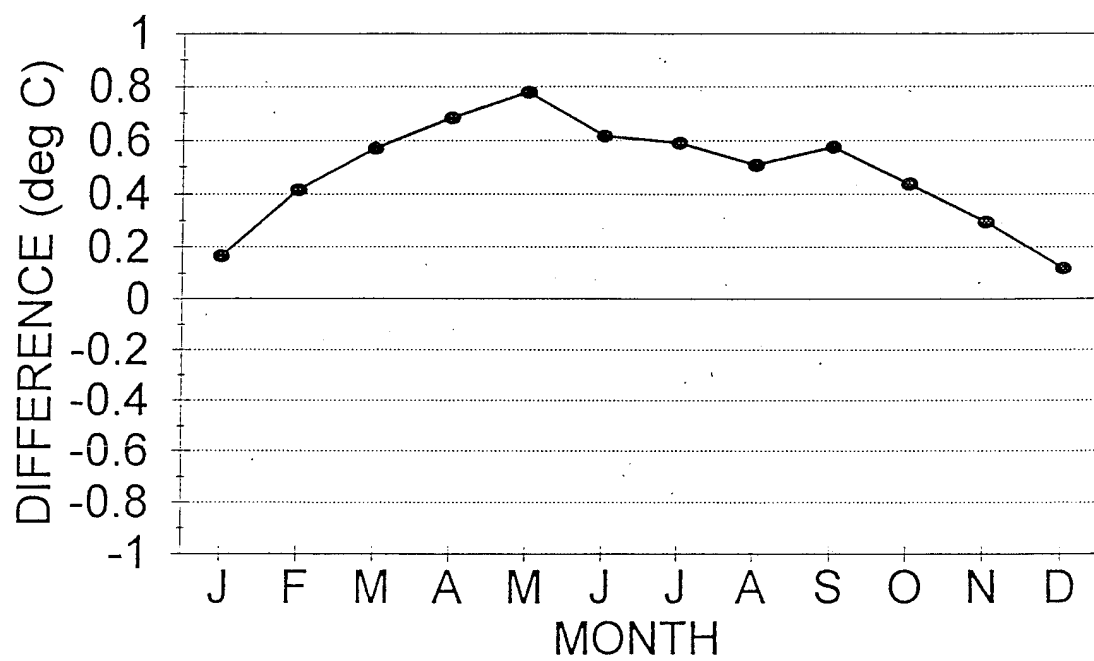


Figure 23. Satellite vs. Reynolds' climatology differences by month for the Indian Ocean.

Table VI. Tropical latitude differences for both Northern and Southern Hemispheres

MONTH	30 N (°C)	20 N (°C)	10 N (°C)	Equator (°C)	10 S (°C)	20 S (°C)	30 S (°C)
JAN	0.453	0.35	0.071	-0.118	0.158	-0.066	-0.157
FEB	0.319	0.265	-0.01	-0.066	0.346	0.398	0.351
MAR	-0.018	0.073	-0.079	0.048	0.478	0.681	0.753
APR	-0.209	-0.065	-0.213	0.057	0.516	0.746	0.904
MAY	-0.446	-0.105	-0.014	0.209	0.55	0.694	0.894
JUN	-0.383	-0.212	-0.102	0.074	0.497	0.631	0.843
JUL	-0.161	-0.18	-0.065	0.014	0.412	0.531	0.723
AUG	-0.143	-0.224	-0.036	-0.044	0.29	0.398	0.55
SEP	0.144	-0.064	-0.044	-0.054	0.218	0.305	0.372
OCT	0.258	-0.059	-0.027	-0.132	0.047	0.08	0.103
NOV	0.429	0.25	0.134	-0.103	0.027	-0.047	-0.267
DEC	0.479	0.301	0.106	-0.167	0.063	-0.169	-0.385

Table VII. High latitude differences for both Northern and Southern Hemispheres

MONTH	60 N (°C)	50 N (°C)	40 N (°C)	40 S (°C)	50 S (°C)	60 S (°C)
JAN	1.322	0.471	0.276	0.222	0.492	0.46
FEB	1.104	0.215	0.044	0.465	0.652	0.474
MAR	1.202	0.218	-0.119	0.846	0.928	0.675
APR	0.798	-0.283	-0.337	0.966	0.743	1
MAY	0.291	-0.372	-0.119	0.875	0.874	1.124
JUN	0.065	-0.362	-0.503	0.755	0.809	1.273
JUL	0.507	-0.151	-0.506	0.755	0.771	1.129
AUG	0.338	0.13	-0.042	0.648	0.772	1.195
SEP	0.411	0.439	0.311	0.498	1.124	1.522
OCT	0.288	0.585	0.512	0.15	1.093	1.485
NOV	0.283	0.313	0.429	-0.008	0.553	1.15
DEC	0.695	0.134	0.32	-0.029	0.358	0.751

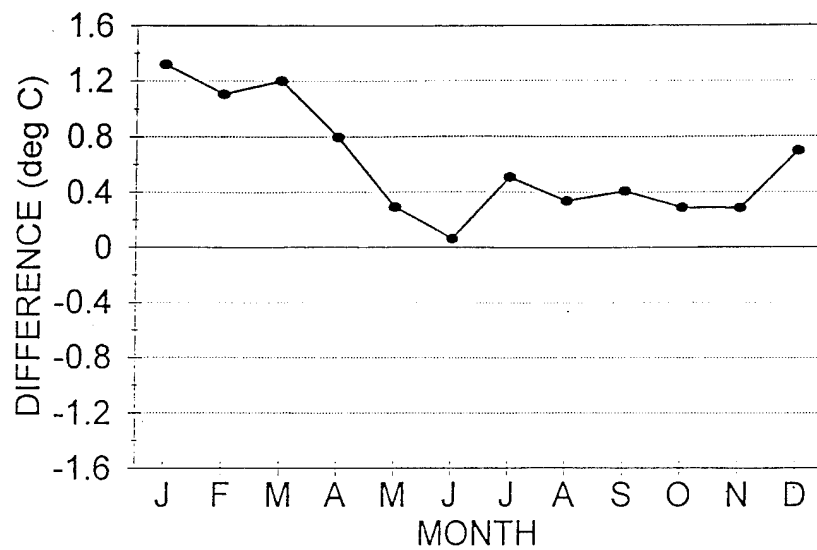


Figure 24. Zonal differences for 60 degrees North.

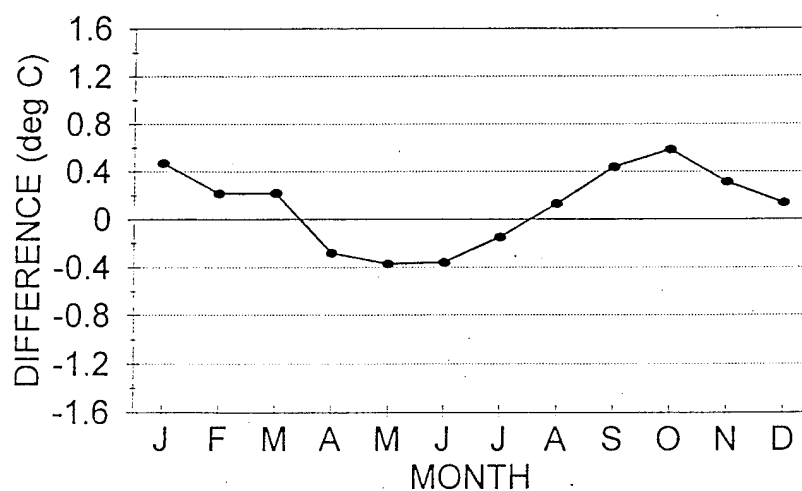


Figure 25. Zonal differences for 50 degrees North.

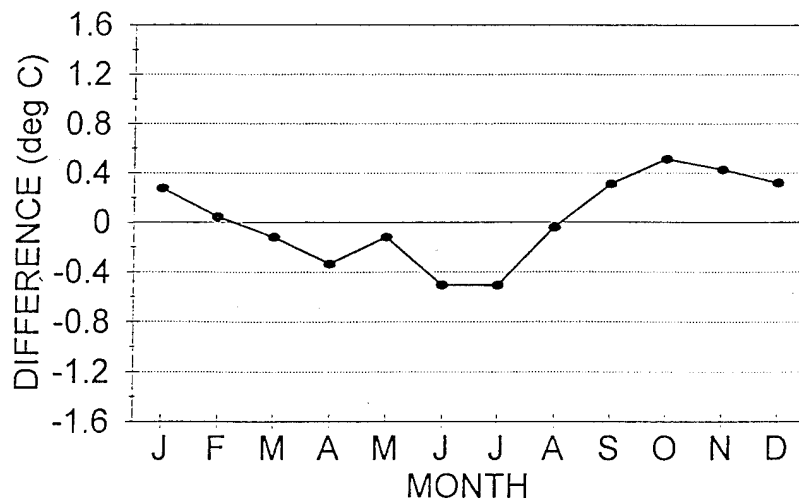


Figure 26. Zonal differences for 40 degrees North.

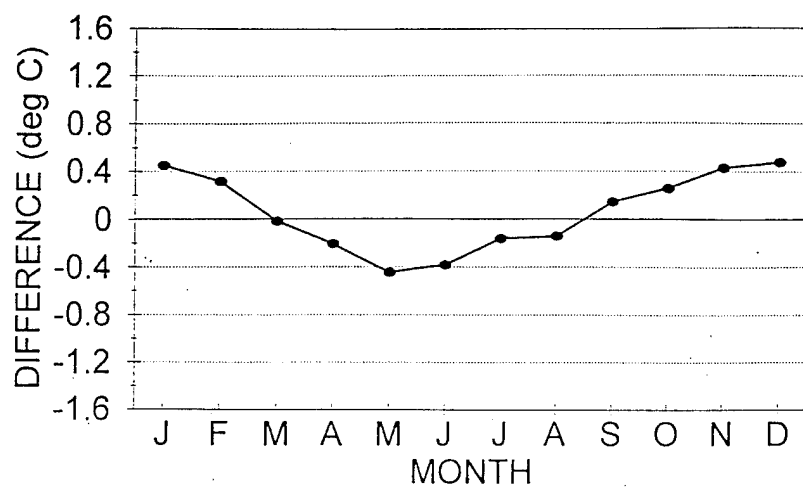


Figure 27. Zonal differences for 30 degrees North.

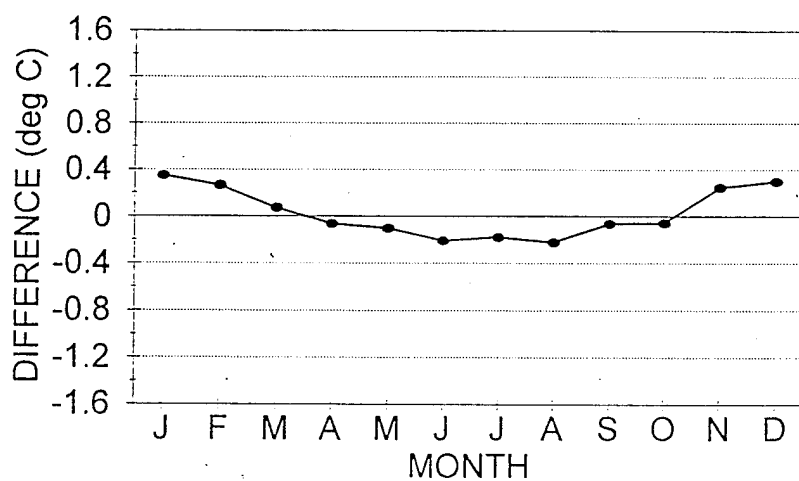


Figure 28. Zonal differences for 20 degrees North.

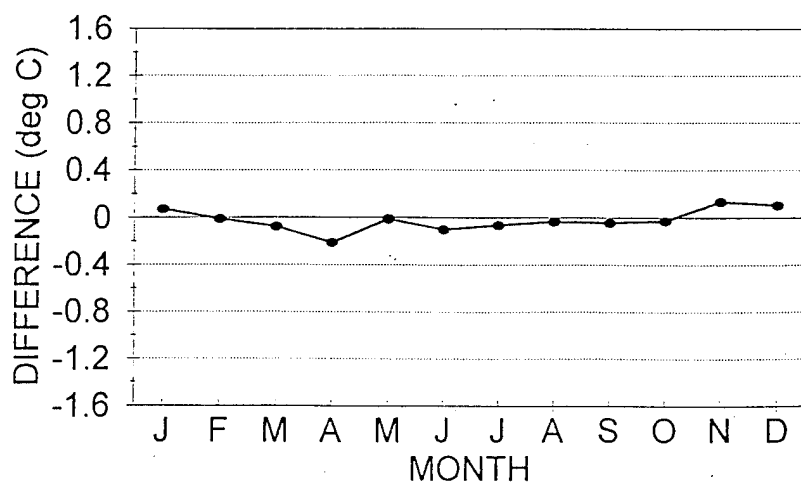


Figure 29. Zonal differences for 10 degrees North.

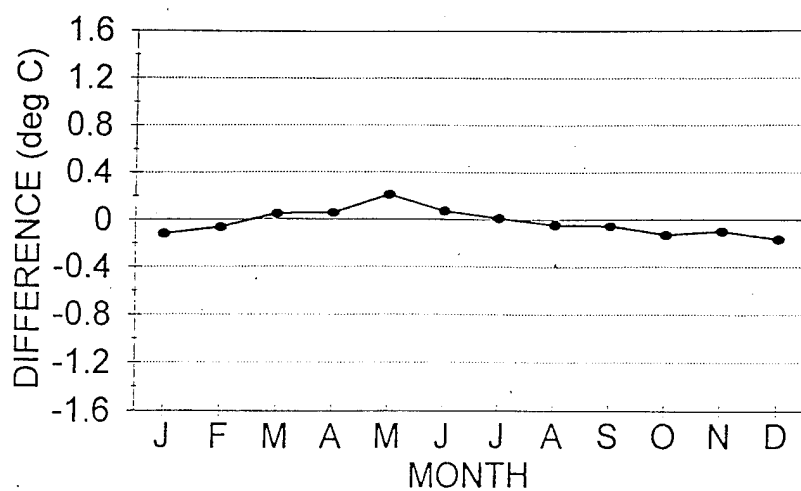


Figure 30. Zonal differences for the Equator.

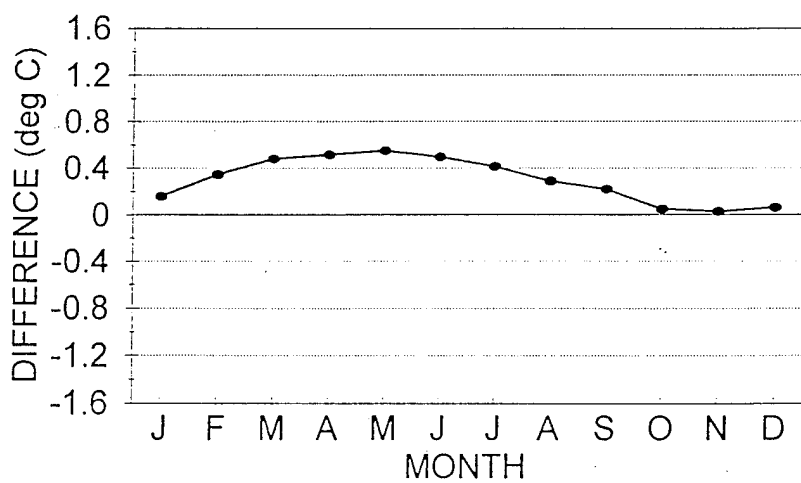


Figure 31. Zonal differences for 10 degrees South.

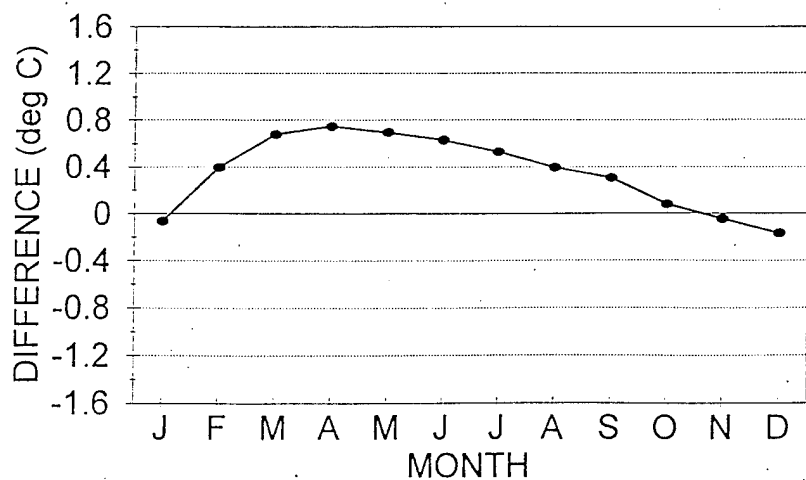


Figure 32. Zonal differences for 20 degrees South.

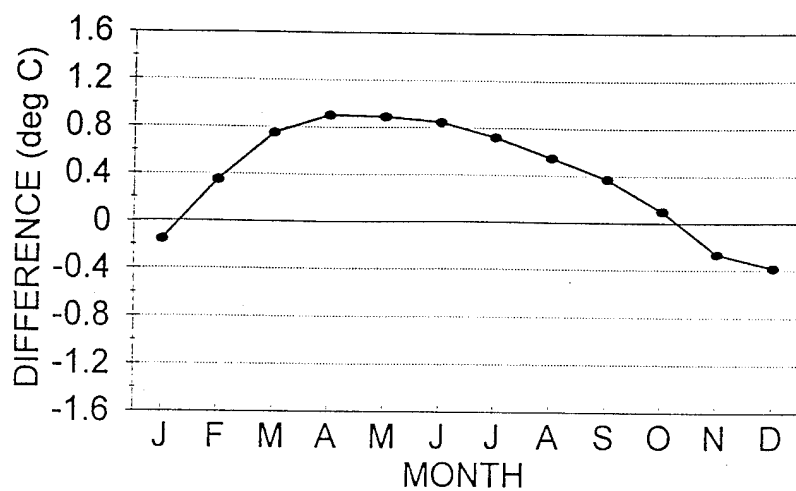


Figure 33. Zonal differences for 30 degrees South.

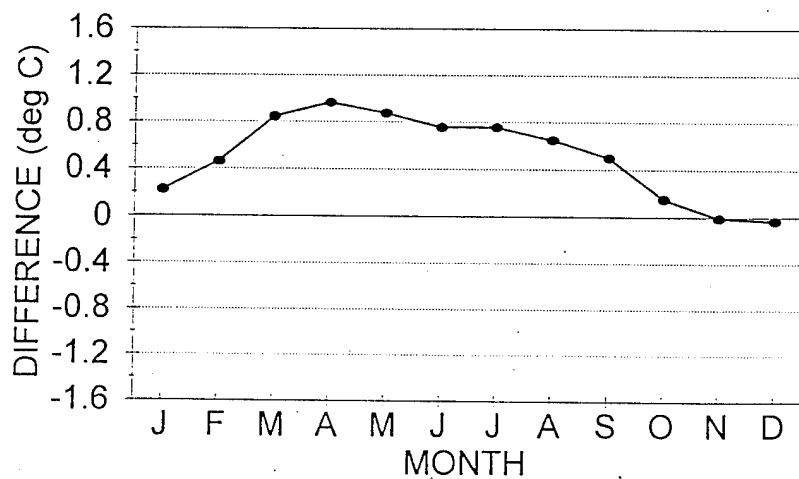


Figure 34. Zonal differences for 40 degrees South.

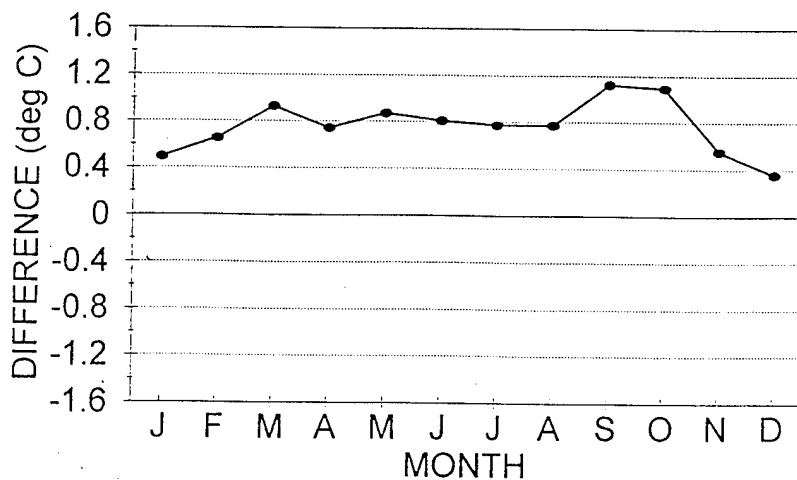


Figure 35. Zonal differences for 50 degrees South.

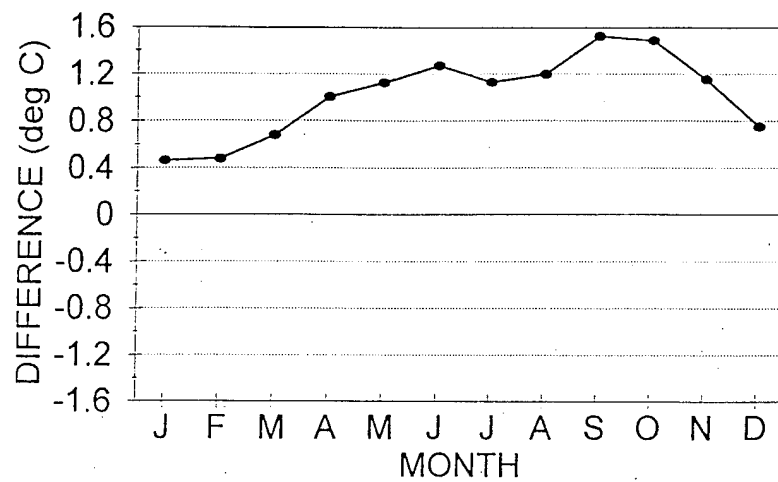


Figure 36. Zonal differences for 60 degrees South.

Special Examinations

Image examinations were undertaken and comparisons of unique ocean characteristics have been made to show the greater accuracy of the MCSST satellite climatology visually. The El Niño of 1987, La Niña of 1988, areas of upwelling, and major current systems all are defined dramatically better within the satellite anomaly product. Development and extent of each of these oceanic characteristics require accurate monitoring since all are intimately linked with global climate prediction. As a result, the satellite climatology, due to its better spatial resolution, should act as a better model for anyone studying climate change, or even studying individual features of the Earth's oceans.

i. El Niño

The El Niño is one of the most unique and influential marine phenomena. It is second only to the change of seasons in its impact on world climate. However, the change of the seasons is easy to predict; the El Niño is not (Wallace, 1994). The El Niño, very basically, is a weakening of trade winds in the Pacific allowing warm water from the western Pacific to flow east. This warm water, which flows all the way to the coast of Peru, suffocates all upwelling along the coast and temporarily destroys the Peruvian fisheries (Wallace, 1994). The El Niño also affects other regions of the globe, as well, through atmospheric teleconnections. The winters following an El Niño are typically mild throughout

western Canada and the northern United States and often rainfall increases significantly over the southern United States. Droughts and fires also typically result in other areas from this climate disruption. Agricultural and fishing loss, flooding, fires, hurricanes, and droughts attributed to the El Niño of 1982-83 led to over 8 billion dollars in damage or loss (Wallace, 1994). Any effort available to improve monitoring and the ultimate prediction of the El Niño should be pursued.

In Figure 37 and 38, one can see that the El Niño of 1987 is much better defined in the anomaly using the new satellite climatology than the Reynolds climatology. Making use of more accurate models will, undoubtedly, improve our predictions on this important marine phenomenon.

ii. La Niña

The La Niña is the process in which normal conditions return to the eastern tropical Pacific after the El Niño. The colder water will once again return to the eastern Pacific as upwelling intensifies along the Peruvian coast. Although there have yet been no proven great economic implications caused by La Niña, it is still important to define in order to help our understanding of the complete equatorial atmospheric/oceanic process. The MCSST anomaly provides a well defined image of the La Niña (Figure 39) in 1988 while the Reynolds anomaly (Figure 40) appears somewhat coarse and less defined.



Figure 37. MCSST vs. Satellite Climatology anomaly of El Niño from April 1987.



Figure 38. MCSST vs. Reynolds' Climatology anomaly of El Niño from April 1987.



Figure 39. MCSST vs. Satellite Climatology anomaly of La Niña in April 1988.



Figure 40. MCSST vs. Reynolds' climatology anomaly of La Niña in April 1988.

iii. Areas of Upwelling

General areas of upwelling play a large role in coastal marine biology and fishery production. Upwelling occurs when surface water moves away from the coastline, either from winds or Coriolis force (force resulting from the Earth's rotation), allowing underlying, colder water to rise and bring nutrients from greater depths. The higher resolution satellite climatology defines such areas with greater accuracy than has been possible previously with the Reynolds product. One particular area is the upwelling in the Gulf of Tehuantepec which occurs off the southern coast of Central America. The images provided, Figures 41 and 42, are the monthly averages of January.

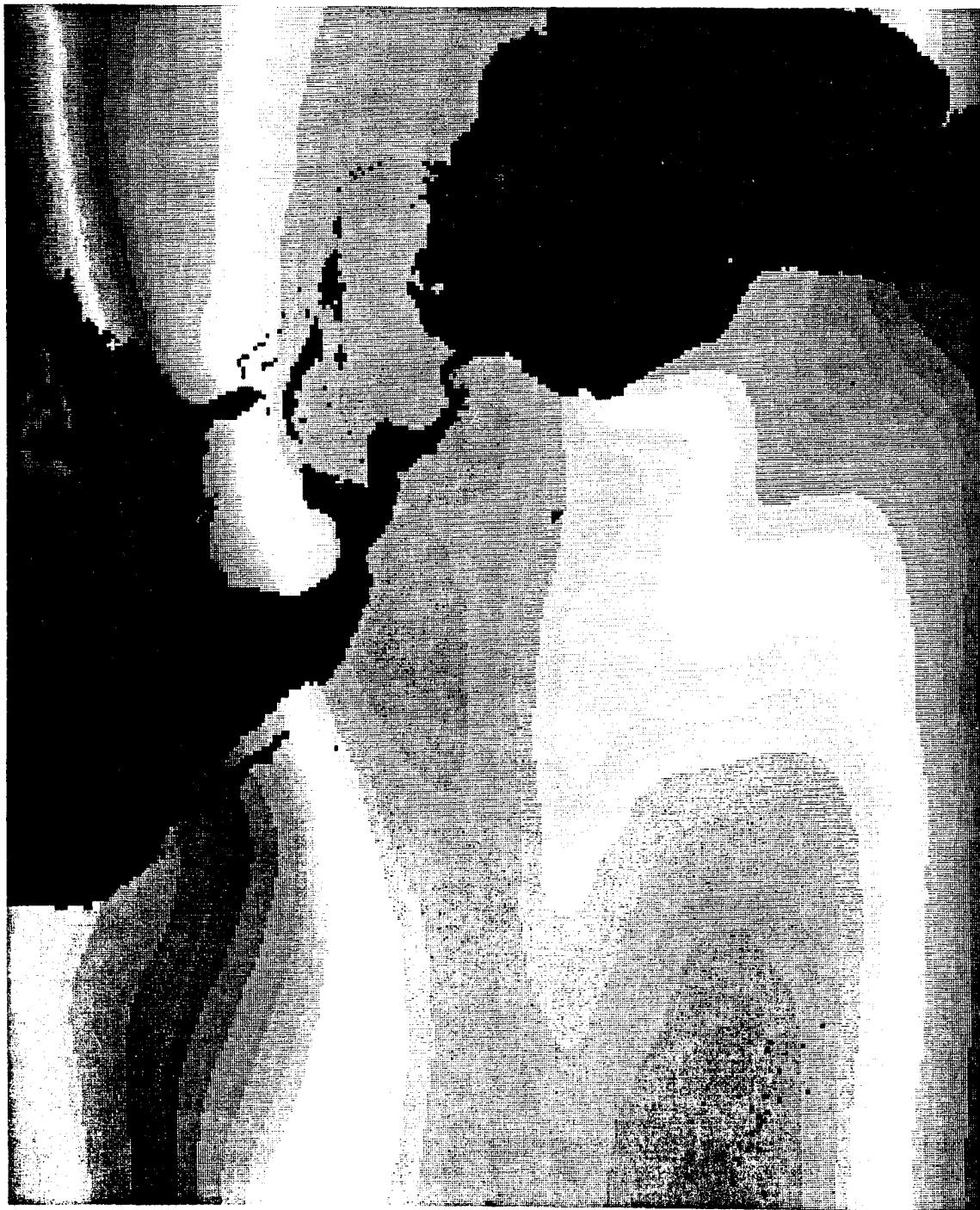
Equatorial upwelling is another area that plays an important role in the biological realm of the ocean. As the circular currents from both the Northern and Southern Hemisphere pass each other, they are respectively deflected to the right and the left by the Coriolis force (Wallace, 1994). As the currents are driven to the west and north by the southeasterly trade winds of the Southern Hemisphere, they "pull" away from each other at the Equator, and the underlying water is forced to rise. This process allows phytoplankton and other small, nutrient life form to thrive along the Equator. The Equatorial upwelling MCSST image (Figure 43) clearly shows cooler water along the Equator, while the Reynolds image (Figure 44) is once again not as well defined.

Note: Scales in all charts are in °C.



16 17 18 19 20 21 22 23 24 25 26 27 28 29 30

Figure 41. MCSST image of Tehuantepec upwelling in January



16 17 18 19 20 21 22 23 24 25 26 27 28 29 30

Figure 42. Reynolds' image of Tehuantepec upwelling in January.



16 17 18 19 20 21 22 23 24 25 26 27 28 29 30

Figure 43. MCSST image of Equatorial upwelling in February.



16 17 18 19 20 21 22 23 24 25 26 27 28 29 30

Figure 44. Reynolds' image of Equatorial upwelling in February.

iv. Current Systems

All major currents within the Earth's oceans play very important roles in global climate change. Currents are not only responsible for the circulation of water through the world's ocean basins, but also for the circulation of heat through the oceans. With this in mind, and recalling that the Earth's heat budget is greatly affected by the oceans (since the oceans cover almost 3/4 of the Earth's surface), it becomes apparent that the migration and change of the major current systems must constantly be monitored. Global climatologies provide excellent models for making continual observations and comparisons of all current systems. Unfortunately, Reynolds' *in-situ* climatology does not provide enough spatial resolution to map anything more than the grossest nature of the major ocean gyres. However, the new satellite climatology does provide more detail in which most currents can be easily identified and evaluated.

In the following pages, there are images of two major currents. The Gulf Stream, Figures 45 and 46, runs north along the eastern seaboard of the United States. The MCSST month image provides a detailed image of the current while that of Reynolds does not even identify it. In Figures 47 and 48, there are images of the Peru Current, which runs northward along the western coast of South America and then turns westward. Once again, the MCSST month image (Figure 47) provides far greater detail and outlines the northern section of the

current where it begins to turn west at the Equator. The Reynolds image (Figure 48) appears too generalized and washes out many of the characteristics of the ocean current.



16 17 18 19 20 21 22 23 24 25 26 27 28 29 30

Figure 45. MCSST image of Gulf Stream for the month of June.



16 17 18 19 20 21 22 23 24 25 26 27 28 29 30

Figure 46. Reynolds' image of the Gulf Stream for the month of June.



16 17 18 19 20 21 22 23 24 25 26 27 28 29 30

Figure 47. MCSST image of the Peru Current for the month of July.

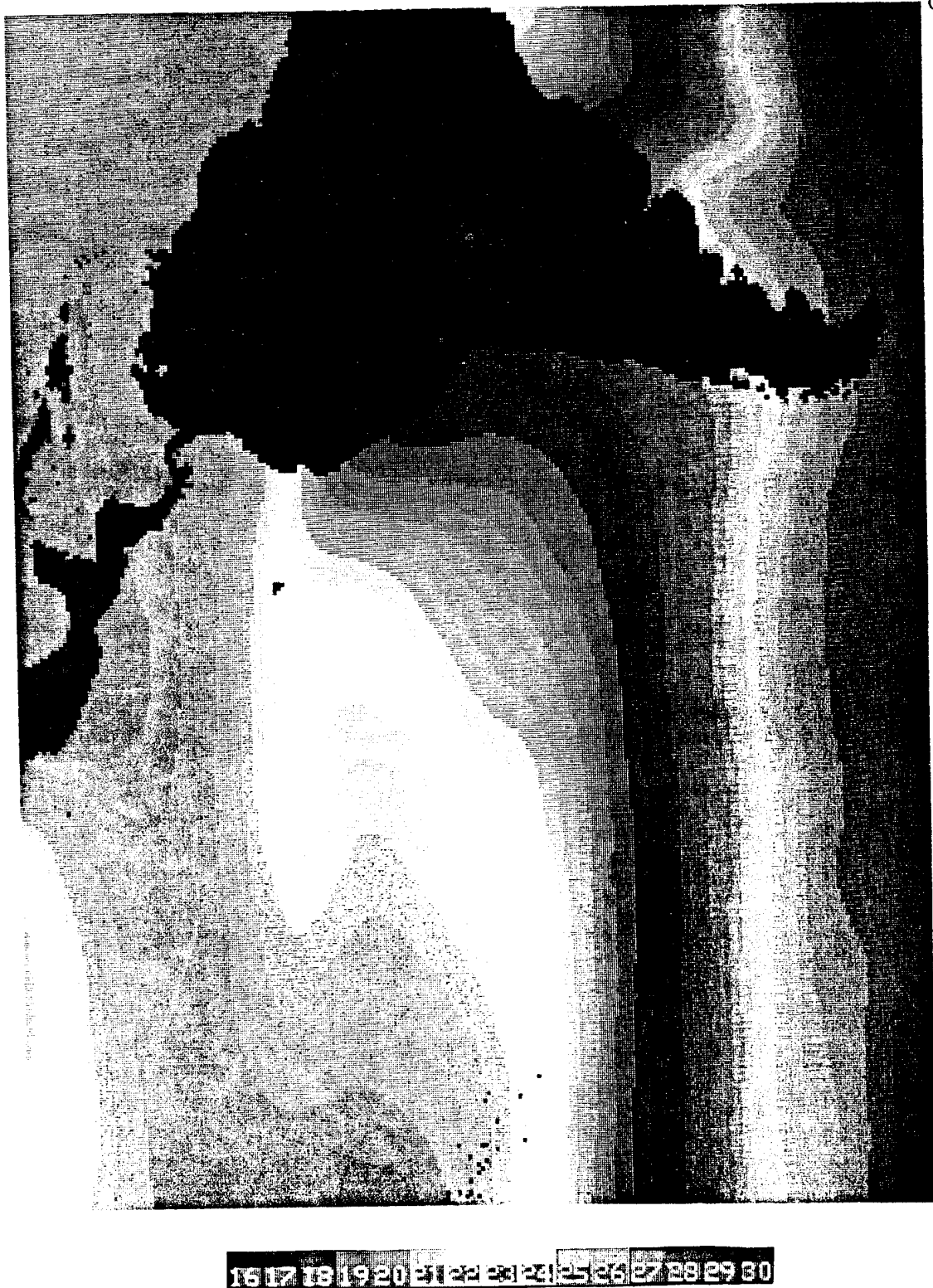


Figure 48. Reynolds' image of the Peru Current for the month of July.

Conclusions

This research has exploited MCSST (multi-channel sea-surface temperature) data to produce a higher resolution ocean sea-surface temperature climatology. When the new 1/3 degree latitude/longitude satellite climatology was compared to the existing NOAA *in-situ* Reynolds climatology, the new monthly anomalies are shown to portray more dramatically improved and more tightly defined fields. Differences between the older operational SST climatology and the newer high-resolution satellite model help illustrate areas of past potential deficiencies from lack of data or inaccurate data. Derived global differences indicate that the sea surface temperature within the satellite climatology is slightly greater (0.27°C) than that of Reynolds. This may be because the 1980's and 1990's have been a warmer time period than the previous three decades. However, regional and zonal differences indicate that this positive difference stems primarily from offsets within the Southern Hemisphere indicating a potential negative bias and notable weakness within Reynolds' climatology.

Use of some marine phenomena, such as El Niño, to highlight comparisons between anomalies produced from both climatologies, reveals dramatic improvements in the anomalies produced from the new MCSST climatology. Also, several current systems and areas of upwelling were shown

to be better defined within the MCSST climatology. Other strengths of the high-resolution satellite climatology are dominated by what is believed to be a more accurate portrayal of the sea surface temperature within the Southern Hemisphere. The creation of an SST climatology must be an on-going process, as the time series grows, in which continual corrections are made so that we continue to better the model of the Earth's oceans and, subsequently, understand our changing climate.

Acknowledgements

I wish to primarily thank my advisors, Drs. A.E. Strong and P.W. Guth, for their constant assistance and guidance. I would also like to thank others who contributed to making this project possible: M. Bem, Dr. D.R. Smith, R.J. Smalley, R.H. Stephens, and my family: Haley, Patrick, Sean, Chris, Mark and Carol Lynn Winter.

References

- Bates, J.J., and H.F. Diaz, 1991. Evaluation of multichannel sea surface temperature product quality for climate monitoring: 1982-1988. *Journal of Geophysical Research*, 96(C11), 20613-20622.
- Gallegos, S.C., and Hawkins, J.D., 1993. A new automated method of cloud masking for AVHRR full-resolution data over the ocean. *Journal of Geophysical Research*, 98(C5), 8505-8516.
- Gleeson, M.W., 1994. Correlation of coral bleaching events and remotely sensed sea surface temperature. Trident Scholar Report #215, U.S. Naval Academy, Annapolis, Maryland, 58 pp.
- Reynolds, R.W., June 1982. A monthly average climatology of sea surface temperature. *NOAA Technical Report*, 31 pp.
- Reynolds, R.W., and D.C. Marsico, 1993. An improved real-time global sea surface temperature analysis. *Journal of Climate*, 6, 114-119.
- Reynolds, R.W., and T.M. Smith, 1994. Improved global sea surface temperature analyses using optimum interpolation. *Journal of Climate*, 4, 1-40.
- Reynolds, R.W., and T.M. Smith, 1995. A high resolution global sea surface temperature climatology. In press, *Journal of Climate*, July 1995.
- Robinson, I.S., *Satellite Oceanography*, Halsted Press, 1985.
- Robinson, M.K., 1976. Atlas of North Pacific Ocean monthly temperatures and mean salinities of the surface layer. Naval Oceanography Ref. Pub. 2, U.S. Navy, Washington D.C.
- Stowe, L.L., and A.E. Strong, 1993. Comparing stratospheric aerosols from El Chicón and Mount Pinatubo using AVHRR data. *Geophysical Research Letters*, 20(12), 1183-1186.
- Strong, A.E., 1984. Monitoring El Chichón aerosol distribution using NOAA-7 satellite AVHRR sea surface temperature observations. *Geofisica Internacional*, 23(2), 129-141.

- Strong, A.E., 1992. Sea surface temperature signals from satellites. In *Encyclopedia of Earth System Science*, Ed. Nierenberg, Academic Press, San Diego, Vol. 4, pp. 69-80.
- Strong, A.E., and E.P. McClain, 1984. Improved ocean surface temperature from space-comparisons with drifting buoys. *Bulletin of the American Meteorological Society*, 65(2), 138-142.
- Wallace, J.M., 1994. El Niño and climate prediction. *Reports to the Nation On Our Changing Planet*, 3, 1-24.
- Watson, C., 1985. Satellite measurement of sea surface temperature in the presence of volcanic aerosols. *Journal of Climate and Applied Meteorology*, 24(6), 501-507.
- Yokoyama, R., and S. Tanba, 1991. Estimation of sea surface temperature via AVHRR of NOAA-9 -- comparison with fixed buoy data. *International Journal of Remote Sensing*, 12(12), 2513-2528.

Glossary of Terms

Algorithm: A mathematical relation between an observed quantity and a variable used in a step-by-step mathematical process to calculate a quantity.

Anomaly: The deviation of sea surface temperature in a given region over a specified period from the normal value for the same region.

AVHRR: Advanced Very High Resolution Radiometer. A five-channel scanning instrument that quantitatively measures electromagnetic radiation. AVHRR is flown on NOAA satellites and determines cloud coverage and surface temperature.

Aerosol: Particles of liquid or solid dispersed as a suspension in the atmosphere.

Climatology: A field or chart of average conditions (eg. SST, currents, salinity) for a specified period of time used for the study of climate and climate phenomena.

Coriolis Force: The apparent tendency of a freely moving particle to swing to one side when its motion is referred to a set of axes that is itself rotating in space, such as Earth.

Difference: Value found after subtracting the monthly averages of the satellite climatology from that of the Reynolds climatology.

Earth's Heat Budget: The emission, absorption, and use of the thermal energy received by the Earth.

El Niño: A warming of the surface waters of the eastern equatorial Pacific due to the weakening of the trade winds. El Niño will occur at irregular intervals of 2-7 years, usually lasting 1-2 years.

In-situ: Latin for "in original place." Refers to measurements made at the actual location of the object measured. For example, sea surface temperature observations made by ships and buoys.

La Niña: Cooler water flows back to the eastern equatorial Pacific signalling the end of an El Niño and a return to normal conditions.

MCSST: Multi-channel sea surface temperature. Observational data collected by the AVHRR.

NOAA: National Oceanographic and Atmospheric Administration

Remote Sensing: The technology of acquiring data and information about an object or phenomena by a device that is not in physical contact with it. A satellite uses remote sensing to gather sea surface temperature data.

Upwelling: Areas of the ocean in which deep water is able to surface bringing nutrients from depths.

SST: Sea surface temperature